Advances in Differential Equations and Control Processes 2026, 33(3), 4577.
doi: https://doi.org/10.59400/adecp4577

Article

Complex dynamics of a tri-trophic predator-prey system with double fear effects

Ting Yang, **Yue Cai***

Department of Mathematics, Jiangxi University of Finance and Economics, Nanchang 330013, China; tyang0315@jxufe.edu.cn
*** Corresponding author:** Yue Cai, caiyue@jxufe.edu.cn

CITATION

Yang T, Cai Y. Complex dynamics of a tri-trophic predator-prey system with double fear effects. Advances in Differential Equations and Control Processes. 2026; 33(3): 4577. https://doi.org/10.59400/adecp4577

ARTICLE INFO

Received: 28 June 2026
Revised: 25 July 2026
Accepted: 13 August 2026
Available online: 21 August 2026

Abstract: In this paper, we investigate a tri-trophic predator-prey system with double fear effects, where the prey is affected by fear induced by both the intermediate predator and the top predator. The top predator is assumed to feed on both the basal prey and the intermediate predator. We establish the positivity and boundedness of solutions and derive sufficient conditions for the global asymptotic stability of axial equilibria. The possible interior equilibria are characterized algebraically, and their local stability is analyzed. We further derive the Hopf bifurcation conditions and compute the first Lyapunov coefficient to determine the direction of the bifurcation and the stability of the bifurcating periodic orbit. Numerical simulations reveal several forms of complex dynamics, including a period-three orbit in the associated return dynamics, the coexistence of a stable equilibrium and a stable limit cycle, the coexistence of two stable limit cycles, and chaotic behavior. The corresponding multistability is further illustrated by basin-of-attraction diagrams. Numerical evidence for chaotic attractors in parameter regions admitting different numbers of interior equilibria is provided by positive largest Lyapunov exponents, parameter bifurcation diagrams, and bounded long-time trajectories. These results show that, within the parameter regimes examined, the interaction between the two fear mechanisms and the tri-trophic feeding structure can generate pronounced dynamical transitions, multistability, and strong sensitivity to initial population densities.

Keywords: predator-prey system; double fear effects; equilibrium; stability; Hopf bifurcation; coexistence; chaos

1. Introduction

Predator-prey interactions are fundamental components of ecological systems and have long been used to understand species persistence, population regulation and community complexity. Since the pioneering works of Lotka and Volterra, classical predator–prey models have been extensively extended by incorporating various ecological mechanisms, such as nonlinear functional responses, stage structure and time delay [1–5]. More recent studies have further considered prey refuge, Allee effects and harvesting [6–8], as well as spatial diffusion and other ecological mechanisms [9–11]. In particular, tri-trophic food-chain models, consisting of a prey, an intermediate predator and a top predator, provide a natural framework for describing energy transfer across trophic levels. Such systems may exhibit richer dynamics than two-species models, including multiple equilibria, periodic oscillations, multistability and chaos [12–15].

Classical predator-prey models usually emphasize the direct consumptive effect of predators on prey. However, ecological evidence shows that predators may also influence prey populations through non-consumptive effects. For example, Brown et al. [16] introduced the concept of the ecology of fear, Preisser et al. [17] emphasized the importance of non-consumptive predator effects, and Zanette et al. [18] experimentally showed that perceived predation risk may reduce reproductive output. These ecological findings have motivated the development of mathematical models incorporating fear effects into predator-prey dynamics. Since then, mathematical studies of fear effects have developed rapidly. Wang et al. [19] proposed a predator-prey model in which predator-induced fear reduces the prey birth rate and showed that fear can alter the system's stability and bifurcation properties. Kumar and Dubey [20] studied a prey-predator system with a fear effect, prey refuge and gestation delay, and investigated the corresponding stability and bifurcation phenomena. Wang and Zou [21] further considered adaptive avoidance of predators and showed that the interaction between fear and delay can produce complicated dynamical behavior. Pal et al. [22] studied a Leslie-Gower predator-prey model with a fear effect and hunting cooperation, where bistability and multiple limit cycles may occur. These works indicate that fear is not merely a biological modification of predation, but also a key mechanism that changes the qualitative dynamics of ecological systems.

Compared with two-species predator-prey models, tri-trophic systems with fear effects are more subtle, because fear may occur at different trophic levels and propagate through the food chain. Panday et al. [23] investigated a three-species food-chain model with fear and showed that fear can significantly affect stability and bifurcation structures. Cong et al. [24] formulated a three-species food-chain model by incorporating the costs and benefits of anti-predator behavior and analyzed its dissipativity, equilibria and long-term dynamics. Kumar and Kumari [25] studied the control of chaos in a three-species food-chain model with a fear effect, showing that the cost of fear may stabilize chaotic dynamics. Rana et al. [26] further considered a three-species food-chain model with fear and an Allee effect and demonstrated the occurrence of complex dynamical phenomena.

Another feature of many ecological communities is that the top predator may not feed exclusively on the intermediate predator. Instead, it may also exploit other lower trophic levels or alternative food sources. This type of feeding structure is closely related to omnivory and intraguild predation, both of which are known to affect food-web stability, persistence and species coexistence [27–31]. Although the present paper does not focus on isolating the independent role of this feeding link, allowing the top predator to feed on both the basal prey and the intermediate predator provides a more flexible tri-trophic interaction structure. Related predator-prey models involving alternative prey, generalist predators, group defense, prey refuge and other ecological mechanisms have been shown to generate Hopf bifurcations, multiple limit cycles, Bogdanov-Takens bifurcations and other complex dynamics [22,32–36].

Motivated by the above studies, we investigate a tri-trophic predator-prey system with double fear effects. The model differs from many existing three-species fear models in two respects. First, the growth of the basal prey is simultaneously reduced by fear induced by the intermediate predator and by the top predator, rather than by a single predator species or a single combined fear term. Second, the top predator consumes both the basal prey and the intermediate predator, so that the double-fear mechanism is coupled with an omnivorous trophic interaction. This formulation provides a framework for examining how predation risk originating from different trophic levels jointly affects population persistence, oscillatory dynamics, and the selection of alternative long-term states.

The main purpose of this paper is to study the stability, bifurcation and complex dynamics of the proposed system. We first establish positivity and boundedness of solutions. Second, we analyze the existence of axial equilibria and establish sufficient conditions for their global stability. Third, we investigate the number and local stability of interior equilibria. Since the interior equilibria cannot always be expressed explicitly in terms of model parameters, the stability analysis is carried out by using the Jacobian matrix and the Routh-Hurwitz criteria. We further determine the Hopf bifurcation condition, verify the transversality condition along the equilibrium branch, and calculate the first Lyapunov coefficient to determine the direction of the Hopf bifurcation and the stability of the bifurcating periodic solutions.

In addition to local bifurcation analysis, we further explore the global dynamical behavior of the system numerically. Our simulations show that the system may exhibit a period-three limit cycle and a non-attracting chaotic set. Since the classical result of Li and Yorke shows that period three implies chaos for one-dimensional continuous maps [37], the observed period-three phenomenon is treated only as an indicator of chaotic dynamics. Moreover, several coexistence phenomena are observed, including the coexistence of a stable equilibrium and a stable limit cycle, as well as the coexistence of two stable limit cycles. These coexistence phenomena are further illustrated by basin-of-attraction diagrams on a two-dimensional section of the initial-condition space. We also find that chaotic attractors may occur in parameter regimes with different numbers of interior equilibria. Claims concerning chaotic sets are supported by phase portraits, time series, positive largest Lyapunov exponents and parameter bifurcation diagrams. These results suggest that double fear effects can induce rich dynamical transitions and complex coexistence patterns in tri-trophic ecological systems.

The rest of this paper is organized as follows. In Section 2, we formulate the model and discuss its basic properties, including positivity and boundedness of solutions. In Section 3, the existence and global stability of axial equilibria are studied. In Section 4, we investigate the number and local stability of interior equilibria. Moreover, we derive the Hopf bifurcation conditions and the first Lyapunov coefficient. Section 5 presents the numerical analysis, including bifurcation diagrams, largest Lyapunov exponents, multistability, basin-of-attraction diagrams, period-three dynamics, and chaotic behavior. Finally, Section 6 gives a brief conclusion and an ecological interpretation of the results.

2. Model

We consider the following tri-trophic predator-prey system

$$\begin{cases} \dfrac{dX}{dT} = RX(1-\dfrac{X}{K})\cdot\dfrac{1}{1+M_1Y+M_2Z} - F_1(X)Y - F_2(X)Z, \\ \dfrac{dY}{dT} = C_1F_1(X)Y - F_3(Y)Z - D_1Y, \\ \dfrac{dZ}{dT} = C_2F_2(X)Z + C_3F_3(Y)Z - D_2Z. \end{cases} \tag{1}$$

Here, $X(T)$, $Y(T)$ and $Z(T)$ denote the population densities of the basal prey, intermediate predator and top predator, respectively. The variable T represents time. The prey population grows logistically with intrinsic growth rate R and carrying capacity K such that $0 < X(T) \leq K$. The term $\dfrac{1}{1+M_1Y+M_2Z}$ describes the reduction in the prey growth rate caused by double fear effects induced by the intermediate predator Y and the top predator Z, where M_1 and M_2 measure the corresponding fear intensities. The functions $F_1(X)$, $F_2(X)$ and $F_3(Y)$ represent functional responses. The constants C_i $(i = 1, 2, 3)$ are conversion rates, and D_1 and D_2 are the natural death rates of the intermediate predator and the top predator, respectively.

In Equation (1), we consider the same Holling type II functional response, namely, $F(M) = F_i(M) = \dfrac{AM}{B+M}$, where A denotes the maximally achievable attack rate and B denotes the half saturation constant. Therefore, one obtains

$$\begin{cases} \dfrac{dX}{dT} = RX(1-\dfrac{X}{K}) \cdot \dfrac{1}{1+M_1Y+M_2Z} - \dfrac{AXY}{B+X} - \dfrac{AXZ}{B+X}, \\ \dfrac{dY}{dT} = \dfrac{C_1AXY}{B+X} - \dfrac{AYZ}{B+Y} - D_1Y, \\ \dfrac{dZ}{dT} = \dfrac{C_2AXZ}{B+X} + \dfrac{C_3AYZ}{B+Y} - D_2Z. \end{cases} \tag{2}$$

Let

$$x = \frac{X}{K},\ y = \frac{Y}{C_1K},\ z = \frac{Z}{C_2K},\ t = RT,$$

then Equation (2) becomes the following nondimensional system

$$\begin{cases} \dfrac{dx}{dt} = x(1-x) \cdot \dfrac{1}{1+m_1y+m_2z} - \dfrac{c_1xy}{B+Kx} - \dfrac{c_2xz}{B+Kx}, \\ \dfrac{dy}{dt} = \dfrac{c_1xy}{B+Kx} - \dfrac{c_2yz}{B+c_1Ky} - d_1y, \\ \dfrac{dz}{dt} = \dfrac{c_2xz}{B+Kx} + \dfrac{c_3yz}{B+c_1Ky} - d_2z, \end{cases} \tag{3}$$

where

$$m_1 = M_1C_1K,\ m_2 = M_2C_2K,\ c_1 = \frac{C_1AK}{R},\ c_2 = \frac{C_2AK}{R},$$

$$c_3 = \frac{C_1C_3AK}{R},\ d_1 = \frac{D_1}{R},\ d_2 = \frac{D_2}{R}.$$

From $0 < X(T) \leq K$, we have $0 < x(t) \leq 1$ holds. Therefore, we consider the dynamics of Equation (3) on the positive invariant region

$$\Omega_+ = \{0 < x \leq 1, y \geq 0, z \geq 0.\}$$

Theorem 1. *All solutions are non-negative and bounded.*

Proof. It follows from Equation (3) that $x = 0$, $y = 0$ and $z = 0$ are invariant algebraic surfaces. Therefore, any solution starting from $(x(0), y(0), z(0))$ is non-negative.

Next, we prove the all solutions are bounded. We divide into two cases: (I) $c_2 \geq c_3$; (II) $c_2 < c_3$.

Case (I). Let $d = \min\{d_1, d_2\}$ and $w = x + y + z$. Then

$$\begin{aligned}\frac{dw}{dt} &= x(1-x)\cdot\frac{1}{1+m_1y+m_2z} - \frac{c_2yz}{B+c_1Ky} + \frac{c_3yz}{B+c_1Ky} - d_1y - d_2z\\ &\le x(1-x) - d_1y - d_2z\\ &\le -dx - dy - dz + (d+1)x\\ &= -dw + (d+1),\end{aligned}$$

which implies that

$$\lim_{t\to\infty}\sup w(t) \le \frac{d+1}{d}.$$

Case (II). Let $d = \min\{d_1, d_2\}$ and $w = x + \frac{c_2}{c_3}y + \frac{c_2^2}{c_3^2}z$. Then

$$\begin{aligned}\frac{dw}{dt} &= x(1-x)\cdot\frac{1}{1+m_1y+m_2z} - \frac{(1-\frac{c_2}{c_3})c_1xy}{B+Kx} - \frac{(1-\frac{c_2^2}{c_3^2})c_2xz}{B+Kx} - \frac{c_2}{c_3}d_1y - \frac{c_2^2}{c_3^2}d_2z\\ &\le x - \frac{c_2}{c_3}d_1y - \frac{c_2^2}{c_3^2}d_2z\\ &\le -dx - d\frac{c_2}{c_3}y - \frac{c_2^2}{c_3^2}dz + (d+1)x\\ &= -dw + (d+1),\end{aligned}$$

which implies that

$$\lim_{t\to+\infty}\sup w(t) \le \frac{d+1}{d}.$$

From Cases (I) and (II), we know that $w(t)$ is bounded. Therefore, all the solutions are bounded. □

3. Global stability of axial equilibria

From Equation (3), we know that $E_0(0,0,0)$ and $E_1(1,0,0)$ are always equilibria.

If $\frac{c_1}{B+K} > d_1$, then Equation (3) has the equilibrium $E_2(x_2, y_2, 0)$, where $x_2 = \frac{d_1B}{c_1 - d_1K}$, $y_2 = \frac{-c_1 + \sqrt{c_1^2 + 4m_1c_1(1-x_2)(B+Kx_2)}}{2m_1c_1}$.

If $\frac{c_2}{B+K} > d_2$, then Equation (3) has the equilibrium $E_3(x_3, 0, z_3)$, where $x_3 = \frac{d_2B}{c_2 - d_2K}$, $z_3 = \frac{-c_2 + \sqrt{c_2^2 + 4m_2c_2(1-x_3)(B+Kx_3)}}{2m_2c_2}$.

Theorem 2. *The equilibrium $E_0(0,0,0)$ is a saddle.*

Proof. The Jacobi matrix at the equilibrium E_0 is

$$J_0 = \begin{pmatrix} 1 & 0 & 0\\ 0 & -d_1 & 0\\ 0 & 0 & -d_2\end{pmatrix},$$

whose eigenvalues are

$$\lambda_1 = 1,\ \lambda_2 = -d_1,\ \lambda_3 = -d_2.$$

Therefore, E_0 is a saddle. □

Theorem 3. *If* $\dfrac{c_1}{B+K} < d_1$ *and* $\dfrac{c_2}{B+K} < d_2$*, then the equilibrium* $E_1(1,0,0)$ *is globally asymptotically stable on* Ω_+.

Proof. The Jacobi matrix at the equilibrium E_1 is

$$J_1 = \begin{pmatrix} -1 & -\dfrac{c_1}{B+K} & -\dfrac{c_2}{B+K} \\ 0 & \dfrac{c_1}{B+K} - d_1 & 0 \\ 0 & 0 & \dfrac{c_2}{B+K} - d_2 \end{pmatrix},$$

whose eigenvalues are

$$\lambda_1 = -1,\ \lambda_2 = \frac{c_1}{B+K} - d_1,\ \lambda_3 = \frac{c_2}{B+K} - d_2.$$

Therefore, if $\dfrac{c_1}{B+K} < d_1$ and $\dfrac{c_2}{B+K} < d_2$, then E_1 is locally asymptotically stable.

Next, we prove that E_1 is globally asymptotically stable.

$$\begin{aligned} \frac{dy}{dt} &= \frac{c_1 xy}{B+Kx} - \frac{c_2 yz}{B+c_1 Ky} - d_1 y \\ &\le \left(\frac{c_1 x}{B+Kx} - d_1\right) y \\ &\le \left(\frac{c_1}{B+K} - d_1\right) y, \end{aligned}$$

which implies that $y(t)$ is monotonically decreasing and satisfies

$$y(t) \le y(0) \exp\left[\left(\frac{c_1}{B+K} - d_1\right) t\right].$$

Therefore, $\lim\limits_{t\to+\infty} y(t) = 0$.

$$\begin{aligned} \frac{dz}{dt} &= \frac{c_2 xz}{B+Kx} + \frac{c_3 yz}{B+c_1 Ky} - d_2 z \\ &\le \left(\frac{c_2}{B+K} - d_2\right) z + \frac{c_3 yz}{B+c_1 Ky} \\ &= \left(\frac{c_2}{B+K} - d_2 + \frac{c_3 y}{B+c_1 Ky}\right) z. \end{aligned}$$

Since $\lim\limits_{t\to+\infty} y(t) = 0$, there exists t_0 such that

$$\frac{c_2}{B+K} - d_2 + \frac{c_3 y(t_0)}{B+c_1 Ky(t_0)} < 0. \tag{4}$$

Therefore, for $t \ge t_0$, we have

$$\begin{aligned} z(t) &\le z(t_0)\cdot\exp\left[\left(\frac{c_2}{B+K} - d_2\right)(t-t_0)\right]\cdot\exp\left[\int_{t_0}^{t}\frac{c_3 y(\tau)}{B+c_1 Ky(\tau)}d\tau\right] \\ &\le z(t_0)\cdot\exp\left[\left(\frac{c_2}{B+K} - d_2 + \frac{c_3 y(t_0)}{B+c_1 Ky(t_0)}\right)(t-t_0)\right]. \end{aligned} \tag{5}$$

Therefore, we have $\lim_{t\to+\infty} z(t) = 0$.

To prove $\lim_{t\to+\infty} x(t) = 1$, we first prove $\limsup_{t\to\infty} x(t) = 1$. We claim that for any $0 < Q < 1$, any $t > 0$, there exists $t_1 > t$ such that $x(t_1) > Q$ holds. If not, then there exist $0 < \bar{Q} < 1$ and $t_2 > 0$ such that $0 < x(t) \le \bar{Q}$ holds for $t \ge t_2$. Since

$$\frac{dx}{dt} = x(1-x)\cdot\frac{1}{1+m_1y+m_2z} - \frac{c_1xy}{B+Kx} - \frac{c_2xz}{B+Kx},$$

we have

$$\begin{aligned}
\frac{dx}{x(1-x)} &= \left(\frac{1}{1+m_1y+m_2z} - \frac{c_1y}{(1-x)(B+Kx)} - \frac{c_2z}{(1-x)(B+Kx)}\right)dt \\
&\ge \left(1-m_1y-m_2z-\frac{c_1y}{(1-x)B}-\frac{c_2z}{(1-x)B}\right)dt \\
&\ge \left(1-m_1y-m_2z-\frac{c_1y}{(1-\bar{Q})B}-\frac{c_2z}{(1-\bar{Q})B}\right)dt \\
&= (1-M_1y-M_2z)\,dt, \qquad (6)
\end{aligned}$$

where $M_1 = m_1 + \dfrac{c_1}{(1-\bar{Q})B}$, $M_2 = m_2 + \dfrac{c_2}{(1-\bar{Q})B}$. Since $\lim_{t\to+\infty} y(t) = 0$ and $\lim_{t\to+\infty} z(t) = 0$, there exists $t_3 > t_2$ such that $1 - M_1y(t) - M_2z(t) > \dfrac{1}{2}$ for $t \ge t_3$. Therefore, from Equation (6), we get

$$\begin{aligned}
\frac{x(t)}{1-x(t)} &\ge \frac{x(t_3)}{1-x(t_3)}\cdot\exp\left[\int_{t_3}^{t}(1-M_1y(\tau)-M_2z(\tau))d\tau\right] \\
&\ge \frac{x(t_3)}{1-x(t_3)}\cdot\exp\left(\frac{1}{2}(t-t_3)\right) \to +\infty \ \ as \ \ t\to+\infty,
\end{aligned}$$

which implies $\lim_{t\to+\infty} x(t) = 1$. This is contradicted with $0 < x(t) \le \bar{Q}$ holding for $t \ge t_2$. Therefore, we have proven our claim, namely, $\limsup_{t\to\infty} x(t) = 1$.

Since E_1 is locally asymptotically stable, there exists $\eta > 0$ such that

$$U_\eta = \{(x,y,z) : |x-1| < \eta,\ 0 \le y < \eta,\ 0 \le z < \eta\}$$

is contained in the basin of attraction of E_1.

Since

$$\lim_{t\to+\infty} y(t) = 0, \qquad \lim_{t\to+\infty} z(t) = 0,$$

there exists $T > 0$ such that

$$y(t) < \eta, \qquad z(t) < \eta, \qquad t \ge T.$$

Choose

$$Q = 1 - \eta.$$

By the claim proved above, for any $t > 0$, there exists $\bar{t} > t$ such that $x(\bar{t}) > Q$. In particular, taking $t > T$, there exists $\bar{t} > T$ such that

$$x(\bar{t}) > 1 - \eta.$$

Since $x(\bar{t}) \leq 1$, it follows that

$$|x(\bar{t}) - 1| < \eta.$$

Consequently,

$$(x(\bar{t}), y(\bar{t}), z(\bar{t})) \in U_\eta.$$

By the local asymptotic stability of E_1, the solution starting from $(x(\bar{t}), y(\bar{t}), z(\bar{t}))$ converges to E_1. Therefore,

$$\lim_{t \to +\infty} (x(t), y(t), z(t)) = (1, 0, 0).$$

Thus, $E_1(1, 0, 0)$ is globally asymptotically stable. □

Theorem 4. *Assume that* $B \geq K$, $\dfrac{c_1}{B+K} > d_1$ *and* $\dfrac{c_2}{B+K} + \dfrac{c_3 Y_*}{B + c_1 K Y_*} < d_2$, *where* $Y_* = 1 + \dfrac{1}{4d_1}$. *Then the equilibrium* $E_2(x_2, y_2, 0)$ *is globally asymptotically stable relative to the interior region*

$$\Omega_+^1 = \{(x, y, z) : 0 < x \leq 1,\ y > 0,\ z \geq 0\}.$$

Proof. The Jacobi matrix J_2 at the equilibrium $E_2(x_2, y_2, 0)$ is

$$\begin{pmatrix} \dfrac{1-2x_2}{1+m_1y_2} - \dfrac{c_1By_2}{(B+Kx_2)^2} & -m_1N_1 - c_1N_2 & -m_2N_1 - c_2N_2 \\ \dfrac{c_1By_2}{(B+Kx_2)^2} & 0 & -\dfrac{c_2y_2}{B+c_1Ky_2} \\ 0 & 0 & \dfrac{c_2x_2}{B+Kx_2} + \dfrac{c_3y_2}{B+c_1Ky_2} - d_2 \end{pmatrix},$$

where $N_1 = \dfrac{x_2(1-x_2)}{(1+m_1y_2)^2}$, $N_2 = \dfrac{x_2}{B+Kx_2}$. The eigenvalues $\lambda_1 = \dfrac{c_2x_2}{B+Kx_2} + \dfrac{c_3y_2}{B+c_1Ky_2} - d_2$ and $\lambda_{2,3}$ satisfy

$$\lambda^2 + \left(\frac{c_1By_2}{(B+Kx_2)^2} - \frac{1-2x_2}{1+m_1y_2}\right)\lambda + \frac{c_1By_2}{(B+Kx_2)^2} \cdot \left(\frac{x_2(1-x_2)m_1}{(1+m_1y_2)^2} + \frac{c_1x_2}{B+Kx_2}\right) = 0.$$

Since $E_2(x_2, y_2, 0)$ is an equilibrium, we have $\dfrac{1-x_2}{1+m_1y_2} = \dfrac{c_1y_2}{B+Kx_2}$. So, if $B \geq K$,

$$\frac{c_1By_2}{(B+Kx_2)^2} - \frac{1-2x_2}{1+m_1y_2} = \frac{x_2(B-K+2Kx_2)}{(1+m_1y_2)(B+Kx_2)} > 0.$$

This implies that $\lambda_{2,3}$ have negative real parts.

Let $W = x + y$, then

$$\begin{aligned} \frac{dW}{dt} &= x(1-x) \cdot \frac{1}{1+m_1y+m_2z} - \frac{c_2xz}{B+Kx} - \frac{c_2yz}{B+c_1Ky} - d_1y \\ &\leq x(1-x) - d_1y \\ &\leq \frac{1}{4} - d_1y. \end{aligned}$$

Since $0 \leq x \leq 1$, $y \geq (W-1)$. Then, we have

$$\frac{dW}{dt} \leq \frac{1}{4} - d_1(W-1) = -d_1 W + d_1 + \frac{1}{4}.$$

This implies that $\limsup_{t\to\infty} W(t) \leq 1 + \frac{1}{4d_1} = Y_*$. In particular,

$$\limsup_{t\to\infty} y(t) \leq Y_*. \tag{7}$$

On the one hand, Equation (7) implies $y_2 \leq Y^*$. Then,

$$\begin{aligned}\lambda_1 =& \frac{c_2 x_2}{B+Kx_2} + \frac{c_3 y_2}{B + c_1 K y_2} - d_2\\ \leq& \frac{c_2}{B+K} + \frac{c_3 Y^*}{B + c_1 K Y^*} - d_2\\ <& 0.\end{aligned}$$

Therefore, the equilibrium E_2 is locally asymptotically stable.

On the other hand, if $\frac{c_2}{B+K} + \frac{c_3 Y_*}{B + c_1 K Y_*} < d_2$, then for some sufficiently small $\epsilon > 0$, $\frac{c_2}{B+K} + \frac{c_3 (Y_* + \epsilon)}{B + c_1 K (Y_* + \epsilon)} < d_2$ holds. Thus, for sufficiently large t, $y(t) < Y_* + \epsilon$ and

$$\begin{aligned}\frac{dz}{dt} &= \frac{c_2 x z}{B+Kx} + \frac{c_3 y z}{B + c_1 K y} - d_2 z\\ &\leq \left(\frac{c_2}{B+K} + \frac{c_3 (Y_* + \epsilon)}{B + c_1 K (Y_* + \epsilon)} - d_2\right) z,\end{aligned}$$

which implies $\lim_{t\to+\infty} z(t) = 0$. Next, we consider the system restricted on the invariant algebraic surface $z = 0$, as follows

$$\begin{cases}\dfrac{dx}{dt} = x(1-x)\cdot\dfrac{1}{1+m_1 y} - \dfrac{c_1 x y}{B+Kx} = f(x,y),\\ \dfrac{dy}{dt} = \dfrac{c_1 x y}{B+Kx} - d_1 y = g(x,y).\end{cases} \tag{8}$$

Choose Dulac function

$$D(x,y) = \frac{B+Kx}{xy}, \quad x > 0, y > 0.$$

Then,

$$D(x,y) f(x,y) = \frac{(B+Kx)(1-x)}{y(1+m_1 y)} - c_1$$

and

$$D(x,y) g(x,y) = c_1 - \frac{d_1(B+Kx)}{x}.$$

Therefore, if $B \geq K$, then

$$\frac{\partial(Df)}{\partial x} + \frac{\partial(Dg)}{\partial y} = \frac{K - B - 2Kx}{y(1+m_1 y)} < 0.$$

According to the Bendixson–Dulac theorem, there exist no periodic orbits in the positive quadrant.

The Equation (8) has three equilibria $O(0,0)$, $O_1(1,0)$ and $O_2(x_2,y_2)$. The eigenvalues of the Jacobi matrices at the equilibria O and O_1 are

$$\Lambda_1 = 1,\ \Lambda_2 = -d_1$$

and

$$\bar{\Lambda}_1 = \frac{c_1}{B+K} - d_1,\ \bar{\Lambda}_2 = -1.$$

If $\dfrac{c_1}{B+K} > d_1$, then $O(0,0)$ and $O_1(1,0)$ are saddles. Further, one could have that the stable manifold and unstable manifold of the saddle O lie on the line $x = 0$ and $y = 0$, respectively. The stable manifold of the saddle O_1 lies on $y = 0$ and the unstable manifold would enter the positive quadrant. Therefore, there exist no closed heteroclinic cycles or homoclinic loops formed by axial equilibria and their connecting orbits.

Note that $\dfrac{c_1}{B+K} > d_1$ and $B \geq K$ implies that $\dfrac{c_1 B y_2}{(B+Kx_2)^2} - \dfrac{1-2x_2}{1+m_1 y_2} > 0$. Therefore, for Equation (8), the unique interior equilibrium $O_2(x_2,y_2)$ is locally asymptotically stable. Besides, all solutions of Equation (8) are bounded. According to the Poincaré-Bendixson theorem, the equilibrium $O_2(x_2,y_2)$ of Equation (8) is globally asymptotically stable on the region $\{(x,y) : 0 < x \leq 1,\ y > 0\}$.

Combine with $\lim\limits_{t\to+\infty} z(t) = 0$, we have that the equilibrium $E_2(x_2,y_2,0)$ of Equation (3) is globally asymptotically stable relative to the interior region Ω_+^1. $\square$

Similar to the proof of Theorem 4, one has the following conclusion.

Theorem 5. *If $B \geq K$, $\dfrac{c_2}{B+K} > d_2$ and $\dfrac{c_1}{B+K} < d_1$. Then the equilibrium $E_3(x_3,0,z_3)$ is globally asymptotically stable relative to the interior region*

$$\Omega_+^2 = \{(x,y,z) : 0 < x \leq 1,\ y \geq 0,\ z > 0\}.$$

4. Interior equilibria and Hopf bifurcation

From Equation (3), the interior equilibrium $E(x,y,z)$ satisfies

$$x(1-x)\cdot\frac{1}{1+m_1y+m_2z} - \frac{c_1xy}{B+Kx} - \frac{c_2xz}{B+Kx} = 0, \tag{9}$$

$$\frac{c_1xy}{B+Kx} - \frac{c_2yz}{B+c_1Ky} - d_1y = 0, \tag{10}$$

$$\frac{c_2xz}{B+Kx} + \frac{c_3yz}{B+c_1Ky} - d_2z = 0. \tag{11}$$

For convenience, we let

$$A(x) = B+Kx,$$

$$U(x) = (c_1 - d_1K)x - d_1B,$$

$$V(x) = d_2B - (c_2 - d_2K)x,$$

and

$$\Delta(x) = c_3 A(x) - c_1 K V(x).$$

From Equations (10) and (11), one gets

$$y = \frac{BV(x)}{\Delta(x)}, \qquad z = \frac{Bc_3 U(x)}{c_2 \Delta(x)}. \tag{12}$$

Then, substitute Equation (12) into Equation (9), we have

$$\begin{aligned} P(x) &:= A(x)(1-x)\Delta^2(x) \\ &\quad - B\big[c_1 V(x) + c_3 U(x)\big]\left[\Delta(x) + Bm_1 V(x) + \frac{Bm_2 c_3}{c_2} U(x)\right] = 0. \end{aligned} \tag{13}$$

Lemma 1. *Define the biologically admissible set*

$$\mathcal{I} = \{x \in (0,1) : U(x) > 0,\ V(x) > 0,\ \Delta(x) > 0\}.$$

Then $E^*(x^*, y^*, z^*)$ is a biologically admissible interior equilibrium if and only if

$$x^* \in \mathcal{I}, \qquad P(x^*) = 0.$$

Consequently, the number of biologically admissible interior equilibria is

$$N_{\text{ad}} = \#\{x \in \mathcal{I} : P(x) = 0\}.$$

Proof. Since $y^* > 0$ and $z^* > 0$, Equations (10) and (11) give

$$\frac{c_2 z^*}{B + c_1 K y^*} = \frac{c_1 x^*}{B + K x^*} - d_1 = \frac{U(x^*)}{A(x^*)} > 0$$

and

$$\frac{c_3 y^*}{B + c_1 K y^*} = d_2 - \frac{c_2 x^*}{B + K x^*} = \frac{V(x^*)}{A(x^*)} > 0.$$

Therefore,

$$U(x^*) > 0, \qquad V(x^*) > 0.$$

Since $y^* > 0$ and $V(x^*) > 0$, it follows that

$$\Delta(x^*) > 0.$$

Moreover, Equation (10) yields

$$\frac{1 - x^*}{1 + m_1 y^* + m_2 z^*} = \frac{c_1 y^* + c_2 z^*}{B + K x^*} > 0.$$

Hence,

$$0 < x^* < 1.$$

Thus $x^* \in \mathcal{I}$. Substitution of y^* and z^* into Equation (10) gives

$$P(x^*) = 0.$$

Conversely, suppose that

$$x^* \in \mathcal{I} \quad \text{and} \quad P(x^*) = 0.$$

Then, from Equation (12), $E^*(x^*, y^*, z^*)$ is an interior equilibrium. This completes the proof. $\square$

From Equation (13), we have

$$c_2 P(x) = A_4 x^4 + A_3 x^3 + A_2 x^2 + A_1 x + A_0 = 0, \tag{14}$$

where

$$\begin{aligned}
A_4 &= -c_2 K^3 (c_3 + c_1(c_2 - d_2 K))^2, \\
A_3 &= c_2 K^2 (c_3 + c_1(c_2 - d_2 K))\Big(- B(3c_3 + c_1(c_2 - 3d_2 K)) + K(c_3 + c_1(c_2 \\
&\quad - d_2 K))\Big), \\
A_2 &= B(-c_1(Bc_2^3 m_1 - c_2^2(2Bd_2 K m_1 + c_3(K - 2BK + (4 + d_1)K^2 + Bm_1)) \\
&\quad - Bc_3 d_1 K(2c_3 + d_2 K)m_2 + c_2 K(c_3^2 + Bd_2^2 K m_1 + c_3 d_2(K - 6BK + (6 \\
&\quad + d_1)K^2 + Bm_1) + Bc_3 d_1 m_2)) + c_3 K(c_2 c_3(3 + d_1)K - B(3c_2 c_3 + c_2^2 d_1 m_1 \\
&\quad - c_2 d_1 d_2 K m_1 + c_3 d_1^2 K m_2)) + c_1^2(c_2^3 K(1 + K) - c_2^2 K(c_3 + 2d_2 K(1 - B + \\
&\quad 2K)) - Bc_3(c_3 + d_2 K)m_2 + c_2(d_2^2 K^3(1 - 3B + 3K) + c_3(d_2 K^2 + Bm_2)))), \\
A_1 &= B^2(-c_1^2 d_2(2c_2^2 K(1 + K) - c_2 K(c_3 + d_2 K(2 - B + 3K)) + Bc_3 m_2) + c_1(c_2^2 \\
&\quad (c_3 + c_3(2 + d_1)K + 2Bd_2 m_1) + 2Bc_3 d_1(c_3 + d_2 K)m_2 - c_2(c_3^2 + 2Bd_2^2 K m_1 \\
&\quad + c_3 d_2(-2(-1 + B)K + 2(3 + d_1)K^2 + Bm_1) + Bc_3 d_1 m_2)) + c_3(c_2 c_3(3 \\
&\quad + 2d_1)K - B(c_2^2 d_1 m_1 + c_2(c_3 - 2d_1 d_2 K m_1) + 2c_3 d_1^2 K m_2))), \\
A_0 &= B^3 c_2 c_3^2 + B^3 c_2 c_3^2 d_1 - B^3 c_1 c_2 c_3 d_2 - 2B^3 c_1 c_2 c_3 d_2 K - B^3 c_1 c_2 c_3 d_1 d_2 K \\
&\quad + B^3 c_1^2 c_2 d_2^2 K + B^3 c_1^2 c_2 d_2^2 K^2 + B^4(c_3 d_1 - c_1 d_2)(c_2 d_2 m_1 - c_3 d_1 m_2).
\end{aligned}$$

Table 1 gives Descartes upper bounds for the number of positive roots of P, where $V(P)$ denotes the number of sign changes in the coefficient sequence of P, and $N_+(P)$ denotes the number of positive real zeros of P, counted with algebraic multiplicity. By Descartes' rule of signs,

$$N_+(P) \le V(P), \qquad V(P) - N_+(P) \in 2\mathbb{N}_0.$$

Table 1. Descartes upper bounds for the number of positive roots of the quartic polynomial $P(x)$.

Sign pattern of $(A_4, A_3, A_2, A_1, A_0)$	$V(P)$	Possible $N_+(P)$	Upper bound for N_{ad}
$(-,-,-,-,-)$	0	0	$N_{\text{ad}} = 0$
$(-,-,-,-,+)$	1	1	$N_{\text{ad}} \le 1$
$(-,-,-,+,-)$	2	2 or 0	$N_{\text{ad}} \le N_+(P) \le 2$
$(-,-,-,+,+)$	1	1	$N_{\text{ad}} \le 1$
$(-,-,+,-,-)$	2	2 or 0	$N_{\text{ad}} \le N_+(P) \le 2$
$(-,-,+,-,+)$	3	3 or 1	$N_{\text{ad}} \le N_+(P) \le 3$
$(-,-,+,+,-)$	2	2 or 0	$N_{\text{ad}} \le N_+(P) \le 2$

Table 1. *Cont.*

Sign pattern of $(A_4, A_3, A_2, A_1, A_0)$	$V(P)$	Possible $N_+(P)$	Upper bound for N_{ad}
$(-,-,+,+,+)$	1	1	$N_{\text{ad}} \leq 1$
$(-,+,-,-,-)$	2	2 or 0	$N_{\text{ad}} \leq N_+(P) \leq 2$
$(-,+,-,-,+)$	3	3 or 1	$N_{\text{ad}} \leq N_+(P) \leq 3$
$(-,+,-,+,-)$	4	4, 2, or 0	$N_{\text{ad}} \leq N_+(P) \leq 4$
$(-,+,-,+,+)$	3	3 or 1	$N_{\text{ad}} \leq N_+(P) \leq 3$
$(-,+,+,-,-)$	2	2 or 0	$N_{\text{ad}} \leq N_+(P) \leq 2$
$(-,+,+,-,+)$	3	3 or 1	$N_{\text{ad}} \leq N_+(P) \leq 3$
$(-,+,+,+,-)$	2	2 or 0	$N_{\text{ad}} \leq N_+(P) \leq 2$
$(-,+,+,+,+)$	1	1	$N_{\text{ad}} \leq 1$

Let $(K, c_1, c_2, c_3, B, d_1, d_2) = (5, 1.2, 1.1, 1, 1, 0.1, 0.2)$. For $m_1 = 1$ and $m_2 = 5$, Equation (3) has unique interior equilibrium $E_1^*(0.96485, 0.01989, 0.10053)$; for $m_1 = 20$ and $m_2 = 10$, the system has two interior equilibria $E_2^*(0.19153, 0.20726, 0.03550)$ and $E_3^*(0.94277, 0.02081, 0.10021)$; for $m_1 = 8$ and $m_2 = 95.5$, the system has three interior equilibria $(0.15653, 0.27248, 0.01286)$, $(0.31526, 0.10762, 0.07008)$ and $(0.62036, 0.04214, 0.09281)$.

Theorem 6. *The interior equilibrium $E(x^*, y^*, z^*)$ is locally asymptotically stable if the condition (17) in the proof holds.*

Proof. The Jacobian matrix at the equilibrium $E(x^*, y^*, z^*)$ is

$$J^* = \begin{pmatrix} J_{11} & J_{12} & J_{13} \\ J_{21} & J_{22} & J_{23} \\ J_{31} & J_{32} & J_{33} \end{pmatrix}, \tag{15}$$

where

$$\begin{aligned}
J_{11} &= \frac{1-2x^*}{1+m_1y^*+m_2z^*} - \frac{c_1By^*}{(B+Kx^*)^2} - \frac{c_2Bz^*}{(B+Kx^*)^2}, \\
J_{12} &= -\frac{x^*(1-x^*)m_1}{(1+m_1y^*+m_2z^*)^2} - \frac{c_1x^*}{B+Kx^*}, \\
J_{13} &= -\frac{x^*(1-x^*)m_2}{(1+m_1y^*+m_2z^*)^2} - \frac{c_2x^*}{B+Kx^*}, \\
J_{21} &= \frac{c_1By^*}{(B+Kx^*)^2}, \qquad J_{22} = \frac{c_1x^*}{B+Kx^*} - \frac{c_2Bz^*}{(B+c_1Ky^*)^2} - d_1, \\
J_{23} &= -\frac{c_2y^*}{B+c_1Ky^*}, \qquad J_{31} = \frac{c_2Bz^*}{(B+Kx^*)^2}, \\
J_{32} &= \frac{c_3Bz^*}{(B+c_1Ky^*)^2}, \quad J_{33} = \frac{c_2x^*}{B+Kx^*} + \frac{c_3y^*}{B+c_1Ky^*} - d_2.
\end{aligned}$$

The eigenvalues $\lambda_i (i = 1, 2, 3)$ satisfies

$$\begin{aligned}
&\lambda^3 - (J_{11}+J_{22}+J_{33})\lambda^2 + (J_{11}J_{22}+J_{11}J_{33}+J_{22}J_{33}-J_{12}J_{21}-J_{13}J_{31} \\
&- J_{23}J_{32})\lambda + (J_{13}J_{22}J_{31} - J_{12}J_{23}J_{31} - J_{13}J_{21}J_{32} + J_{11}J_{23}J_{32} + J_{12}J_{21}J_{33} \\
&- J_{11}J_{22}J_{33}) = 0.
\end{aligned} \tag{16}$$

Let

$$
\begin{aligned}
&Q_1 = -(J_{11} + J_{22} + J_{33}),\\
&Q_2 = J_{11}J_{22} + J_{11}J_{33} + J_{22}J_{33} - J_{12}J_{21} - J_{13}J_{31} - J_{23}J_{32},\\
&Q_3 = J_{13}J_{22}J_{31} - J_{12}J_{23}J_{31} - J_{13}J_{21}J_{32} + J_{11}J_{23}J_{32} + J_{12}J_{21}J_{33} - J_{11}J_{22}J_{33}.
\end{aligned}
$$

Then, we have determinants

$$
\Delta_1 = Q_1,\ \ \Delta_2 = \begin{vmatrix} Q_1 & 1 \\ Q_3 & Q_2 \end{vmatrix} = Q_1Q_2 - Q_3,\ \ \Delta_3 = \begin{vmatrix} Q_1 & 1 & 0 \\ Q_3 & Q_2 & Q_1 \\ 0 & 0 & Q_3 \end{vmatrix} = Q_3\Delta_2.
$$

By Routh-Hurwitz stability criterion, we know that $\lambda_i(i = 1, 2, 3)$ have negative real parts if

$$
\Delta_1 > 0,\ \ \Delta_2 > 0,\ \ \Delta_3 > 0. \tag{17}
$$

Therefore, the equilibrium E is locally asymptotically stable. □

For $(K, m_1, m_2, c_1, c_2, c_3, B, d_1, d_2) = (5, 1, 85, 1.2, 1.1, 1, 1, 0.1, 0.2)$ and the equilibrium $E_4^*(0.7033, 0.03469, 0.09540)$, we have that the condition (17) holds and the eigenvalues of the Jacobi matrix at E_4^* are

$$
\lambda_1 = -0.02852,\ \lambda_{2,3} = -0.0041 \pm 0.05832\mathrm{i}.
$$

Therefore, the unique equilibrium E_4^* is locally asymptotically stable.

Next, we investigate the Hopf bifurcation at the interior equilibrium. Fix m_j $(j \neq i)$ and take $\mu = m_i$ as the bifurcation parameter. Define

$$
H(\mu) = Q_1(\mu)Q_2(\mu) - Q_3(\mu).
$$

and μ^* satisfying $H(\mu^*) = 0$. Suppose that Equation (3) has a branch of biologically admissible interior equilibria

$$
E(\mu) = \big(x^*(\mu), y^*(\mu), z^*(\mu)\big)
$$

in a neighborhood of $\mu = \mu^*$.

Theorem 7. *Assume that*

$$
Q_1(\mu^*) > 0, \qquad Q_2(\mu^*) > 0, \qquad H(\mu^*) = 0,
$$

and

$$
H'(\mu^*) = Q_1'(\mu^*)Q_2(\mu^*) + Q_1(\mu^*)Q_2'(\mu^*) - Q_3'(\mu^*) \neq 0,
$$

where the primes denote total derivatives along the equilibrium branch $E(\mu)$. Then Equation (3) undergoes a Hopf bifurcation at $E(\mu^*)$ as μ passes through μ^*. Furthermore, we have the following statement.

(1) If the first Lyapunov coefficient $l_1 < 0$, then the Hopf bifurcation is

supercritical and a stable bifurcating periodic solution exists for $H'(\mu^*)(\mu - \mu^*) < 0$.

(2) If $l_1 > 0$, *the Hopf bifurcation is subcritical and an unstable bifurcating periodic solution exists for* $H'(\mu^*)(\mu - \mu^*) > 0$.

Proof. Let

$$\lambda^3 + Q_1(\mu)\lambda^2 + Q_2(\mu)\lambda + Q_3(\mu) = 0 \tag{18}$$

be the characteristic equation of the Jacobian matrix evaluated along this equilibrium branch. At $\mu = \mu^*$, the condition

$$H(\mu^*) = Q_1(\mu^*)Q_2(\mu^*) - Q_3(\mu^*) = 0$$

implies that the characteristic polynomial can be factorized as

$$\begin{aligned} p(\lambda, \mu^*) &= \lambda^3 + Q_1(\mu^*)\lambda^2 + Q_2(\mu^*)\lambda + Q_3(\mu^*) \\ &= \big(\lambda + Q_1(\mu^*)\big)\big(\lambda^2 + Q_2(\mu^*)\big). \end{aligned}$$

Since $Q_1(\mu^*) > 0$ and $Q_2(\mu^*) > 0$, the eigenvalues are

$$\lambda_1 = -Q_1(\mu^*) < 0, \qquad \lambda_{2,3} = \pm \mathrm{i}\omega_0,$$

where $\omega_0 = \sqrt{Q_2(\mu^*)} > 0$. Thus, the Jacobian matrix has a pair of purely imaginary eigenvalues and one negative real eigenvalue.

Let

$$\lambda(\mu) = \alpha(\mu) + \mathrm{i}\omega(\mu)$$

denote the eigenvalue branch satisfying $\lambda(\mu^*) = i\omega_0$. Differentiating

$$\lambda^3 + Q_1(\mu)\lambda^2 + Q_2(\mu)\lambda + Q_3(\mu) = 0$$

with respect to μ gives

$$\big(3\lambda^2 + 2Q_1\lambda + Q_2\big)\lambda' + Q_1'\lambda^2 + Q_2'\lambda + Q_3' = 0.$$

Therefore,

$$\lambda' = -\frac{Q_1'\lambda^2 + Q_2'\lambda + Q_3'}{3\lambda^2 + 2Q_1\lambda + Q_2}.$$

Evaluating this expression at $\mu = \mu^*$, $\lambda = \mathrm{i}\omega_0$, and taking the real part, we obtain

$$\frac{d}{d\mu}\operatorname{Re}\lambda(\mu)\bigg|_{\mu=\mu^*} = -\frac{Q_1'(\mu^*)Q_2(\mu^*) + Q_1(\mu^*)Q_2'(\mu^*) - Q_3'(\mu^*)}{2\big(Q_1^2(\mu^*) + Q_2(\mu^*)\big)}.$$

Then, if $H'(\mu^*) = Q_1'(\mu^*)Q_2(\mu^*) + Q_1(\mu^*)Q_2'(\mu^*) - Q_3'(\mu^*) \neq 0$, the transversality condition

$$\frac{d}{d\mu}\operatorname{Re}\lambda(\mu)\bigg|_{\mu=\mu^*} \neq 0$$

holds. Hence, Equation (3) undergoes a Hopf bifurcation at $E(\mu^*)$ as μ passes through μ^*.

Furthermore, we get the first Lyapunov coefficient l_1, see **Appendix A** for the detailed computation. Besides, the radial normal form on the center manifold is

$$\dot{\rho} = \rho\left[\alpha'(\mu^*)(\mu-\mu^*) + l_1\rho^2 + O\big(|\mu-\mu^*|^2+\rho^4\big)\right].$$

Consequently,

$$\begin{aligned}\rho^2 =& -\frac{\alpha'(\mu^*)}{l_1}(\mu-\mu^*) + o(|\mu-\mu^*|).\\ =&\frac{H'(\mu^*)}{2\big(Q_1^2(\mu^*)+Q_2(\mu^*)\big)l_1}(\mu-\mu^*) + o(|\mu-\mu^*|).\end{aligned}$$

Therefore, if $l_1 < 0$, then the Hopf bifurcation is supercritical and a stable bifurcating periodic solution exists for $H'(\mu^*)(\mu-\mu^*) < 0$. If $l_1 > 0$, the Hopf bifurcation is subcritical and an unstable bifurcating periodic solution exists for $H'(\mu^*)(\mu-\mu^*) > 0$. □

Remark 1. *Here, $Q_j'(\mu)$ denotes the total derivative of Q_j along the biologically admissible equilibrium branch $E(\mu)$, namely,*

$$\begin{aligned}Q_j'(\mu) =& \frac{d}{d\mu}Q_j\big(x^*(\mu), y^*(\mu), z^*(\mu), \mu\big)\\ =&\frac{\partial Q_j}{\partial \mu} + \frac{\partial Q_j}{\partial x^*}\frac{dx^*}{d\mu} + \frac{\partial Q_j}{\partial y^*}\frac{dy^*}{d\mu} + \frac{\partial Q_j}{\partial z^*}\frac{dz^*}{d\mu}, \qquad j=1,2,3.\end{aligned}$$

To verify the result, we give the following simulations.

Let $\mu = m_2$ be the bifurcation parameter. For $(K, m_1, c_1, c_2, c_3, B, d_1, d_2) = (1, 1, 1, 0.3, 1.8, 2, 0.1, 0.4)$, by $H(\mu^*) = 0$, we get $\mu^* = 1.0472$ and the unique interior equilibrium $E^*(0.4208, 0.4791, 0.6100)$. Furthermore, $Q_1(\mu^*) = 0.1369 > 0$, $Q_2(\mu^*) = 0.06267 > 0$ and $H'(\mu^*) = -0.002762 < 0$. Therefore, a Hopf bifurcation occurs as μ passes through $\mu^* = 1.0472$. Besides, the first Lyapunov coefficient $l_1 = -1.1562 < 0$, then the Hopf bifurcation is supercritical and a stable limit cycle exists for $\mu > \mu^*$, see **Figure 1b**. When $\mu < \mu^*$, the equilibrium E is stable, see **Figure 1a**.

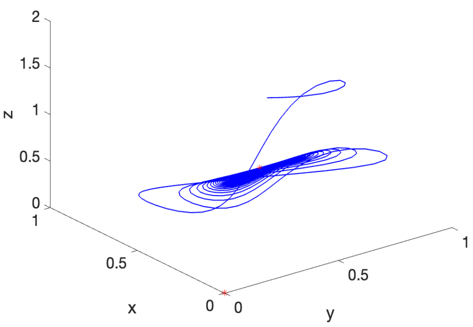

(a)

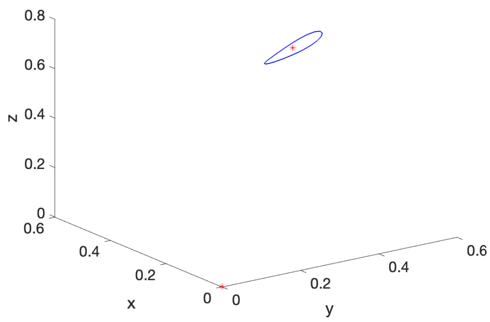

(b)

Figure 1. Phase portrait near E of Equation (3) with $(K, m_1, c_1, c_2, c_3, B, d_1, d_2) = (1, 1, 1, 0.3, 1.8, 2, 0.1, 0.4)$ and different value of m_2: **(a)** $m_2 = 1.03$; **(b)** $m_2 = 1.05$.

Let $\mu = m_1$ be the bifurcation parameter. For $(K, m_2, c_1, c_2, c_3, B, d_1, d_2) = (1, 1, 1, 0.3, 1.8, 2, 0.1, 0.4)$, by $H(\mu^*) = 0$, we get $\mu^* = 0.8992$ and the unique interior equilibrium $E^*(0.4311, 0.4773, 0.6386)$. Furthermore, $Q_1(\mu^*) = 0.14489 > 0$, $Q_2(\mu^*) = 0.06341 > 0$ and $H'(\mu^*) = 0.001405 > 0$. Therefore, a Hopf bifurcation occurs as μ passes through $\mu^* = 0.8992$. Besides, the first Lyapunov coefficient $l_1 = -1.0712 < 0$, then the Hopf bifurcation is supercritical and a stable limit cycle exists for $\mu < \mu^*$, see **Figure 2a**. When $\mu > \mu^*$, the equilibrium E is stable, see **Figure 2b**.

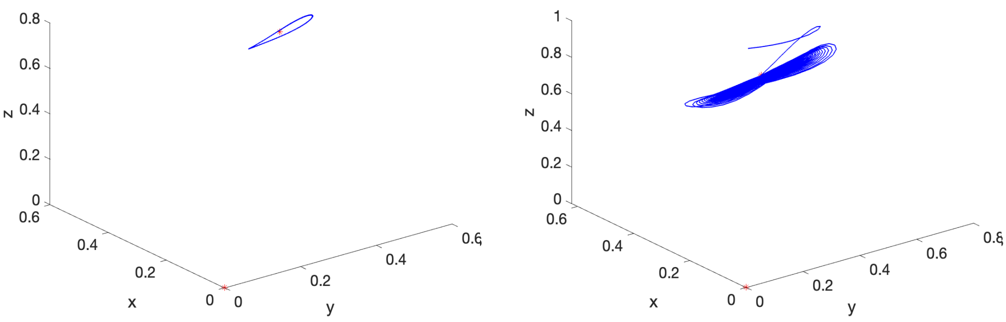

(a) **(b)**

Figure 2. Phase portrait near E of Equation (3) with $(K, m_2, c_1, c_2, c_3, B, d_1, d_2) = (1, 1, 1, 0.3, 1.8, 2, 0.1, 0.4)$ and different value of m_1: **(a)** $m_1 = 0.89$; **(b)** $m_1 = 0.92$.

5. Numerical simulation

In this section, numerical simulations are carried out to explore the complex dynamics of the system. We show that the system may exhibit a period-three limit cycle and a non-attracting chaotic set. Various coexistence phenomena are also observed, including the coexistence of a stable equilibrium and a stable limit cycle, as well as the coexistence of two stable limit cycles. Furthermore, our simulations indicate that chaotic attractors may arise in parameter regimes corresponding to different numbers of interior equilibria. Biologically, these findings indicate that double fear effects can substantially alter the long-term behavior of the food chain, promoting diverse dynamical patterns and ecological outcomes.

5.1. Period-three limit cycle and non-attracting chaotic set

Let $(K, m_1, m_2, c_1, c_2, c_3, B, d_1, d_2) = (5, 0.1, 4.6, 1.425, 1.1, 1.2, 1, 0.1, 0.2)$. Choosing the initial point $(0.5,\ 0.2, 0.5)$, we find that the system has a stable limit cycle, and give the corresponding Poincaré mappings (the cross section $x = 0.9$), as shown in **Figure 3**. Therefore, the Poincaré return map has a period-three orbit.

For one-dimensional continuous maps, the existence of a period-three orbit implies Li-Yorke chaos. However, for a two-dimensional discrete system, a period-three orbit alone does not necessarily guarantee Li-Yorke chaos. Interestingly, we find that the system could show the transient chaos phenomenon, which implies that the system indeed possesses a non-attracting chaotic set, see **Figure 4**. Moreover, we give the time series of the variable $z(t)$, see **Figure 5**. As shown in the figure, the system initially undergoes a period of irregular motion, eventually transitioning to periodic motion.

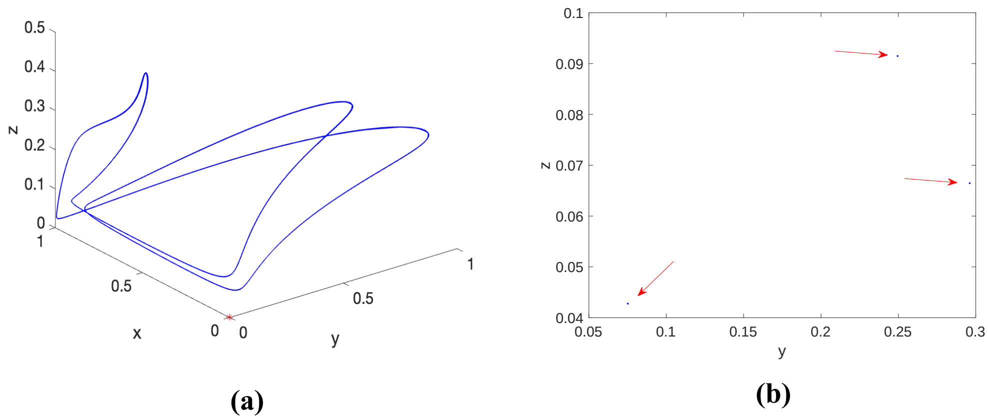

Figure 3. Equation (3) with $(K, m_1, m_2, c_1, c_2, c_3, B, d_1, d_2) = (5, 0.1, 4.6, 1.425, 1.1, 1.2, 1, 0.1, 0.2)$: **(a)** a period-three limit cycle; **(b)** the corresponding Poincaré mappings.

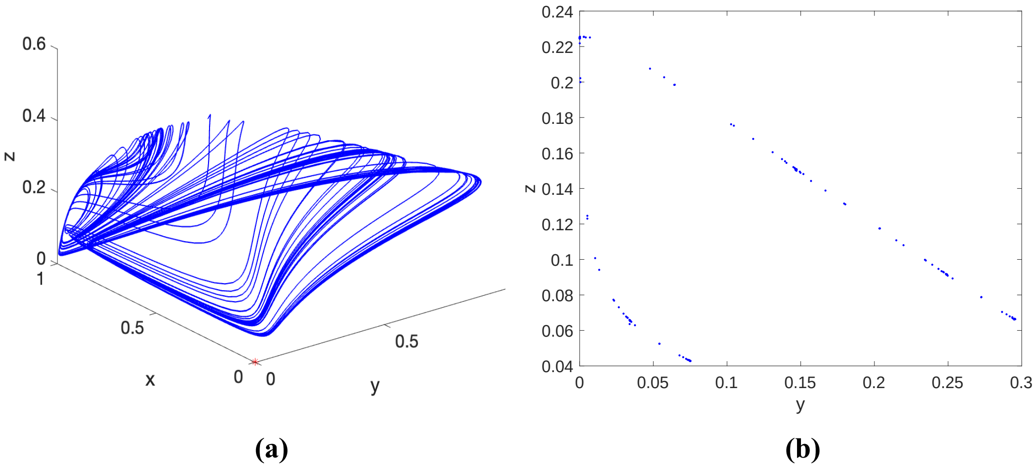

Figure 4. Equation (3) with $(K, m_1, m_2, c_1, c_2, c_3, B, d_1, d_2) = (5, 0.1, 4.6, 1.425, 1.1, 1.2, 1, 0.1, 0.2)$: **(a)** a non-attracting chaotic set; **(b)** its corresponding Poincaré mappings.

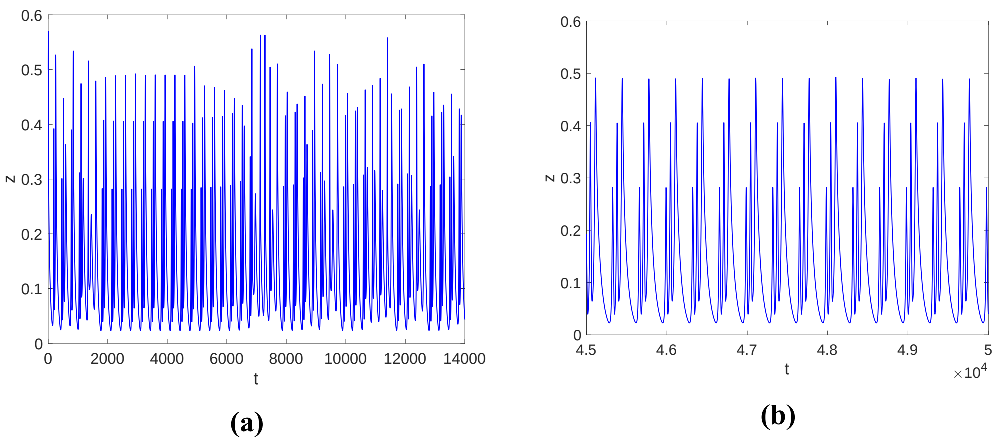

Figure 5. Time series of the variable $z(t)$ of Equation (3) with $(K, m_1, m_2, c_1, c_2, c_3, B, d_1, d_2) = (5, 0.1, 4.6, 1.425, 1.1, 1.2, 1, 0.1, 0.2)$: **(a)** $t \in [0, 14, 000]$; **(b)** $t \in [45, 000, 50, 000]$.

Figure 6 give the finite-time largest Lyapunov exponent convergence after transient removal. In **Figure 6**, the system initially has a positive Lyapunov exponent, which eventually becomes zero over time. Here, the largest Lyapunov exponent was computed using the one-vector Benettin algorithm. The original system and the variational equation were integrated simultaneously using the adaptive MATLAB solver `ode45`. The relative and absolute tolerances were set to 10^{-10} and 10^{-12}, respectively, and the maximum internal step size was restricted to 0.05. A transient interval of length $T_{\text{tr}} = 2,000$ was discarded before the Lyapunov exponent was accumulated. The tangent vector was renormalized every $\Delta T = 1$, and the finite-time largest Lyapunov exponent was computed as

$$\lambda_{\max}(T_N) = \frac{1}{T_N} \sum_{k=1}^{N} \log \rho_k,$$

where ρ_k is the norm of the tangent vector immediately before the k-th renormalization. All these might provide numerical evidence for complex chaotic dynamics.

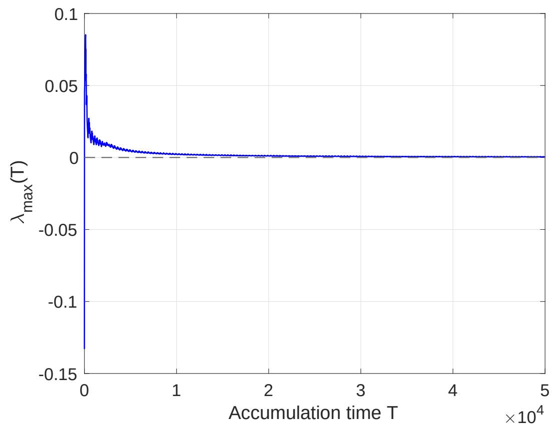

Figure 6. Finite-time largest Lyapunov exponent convergence with $(K, m_1, m_2, c_1, c_2, c_3, B, d_1, d_2) = (5, 0.1, 4.6, 1.425, 1.1, 1.2, 1, 0.1, 0.2)$.

5.2. Multistability

5.2.1. The coexistence of a stable interior equilibrium and a stable limit cycle

Let $(K, m_1, c_1, c_2, c_3, B, d_1, d_2) = (5, 1, 1.2, 1.1, 1, 1, 0.1, 0.2)$ and $m_2 = 55$. In this case, Equation (3) has a unique interior equilibrium $(0.8244, 0.02662, 0.09820)$, and the corresponding eigenvalues are $-0.09148, -0.0009774 \pm 0.04542\text{i}$. This implies that the unique interior equilibrium is stable. Moreover, we find that the system could have a stable limit cycle. Therefore, Equation (3) has the coexistence of a stable interior equilibrium and a stable limit cycle, see **Figure 7**, where the initial points are $(0.8, 0.2, 0.1)$ and $(0.5, 0.5, 0.1)$, respectively.

Figure 8 shows the basin-of-attraction diagrams on four two-dimensional initial-condition sections. The red and blue regions correspond to initial conditions converging to the stable limit cycle and the stable equilibrium, respectively. For $z(0) = 0.1$, the basin of the stable equilibrium occupies a substantial part of the lower region of the $(x(0), y(0))$-plane. As $z(0)$ increases, this basin gradually contracts. At $z(0) = 0.34$, only a small set of initial conditions with relatively low $y(0)$ converges to the equilibrium. For $z(0) = 0.4$, all sampled initial conditions on the considered section converge to the stable limit cycle. These results demonstrate that the relative basin sizes of the coexisting attractors depend strongly on the initial density of the top predator. In particular, larger values of $z(0)$ favor convergence to the oscillatory state within the initial-condition region examined here.

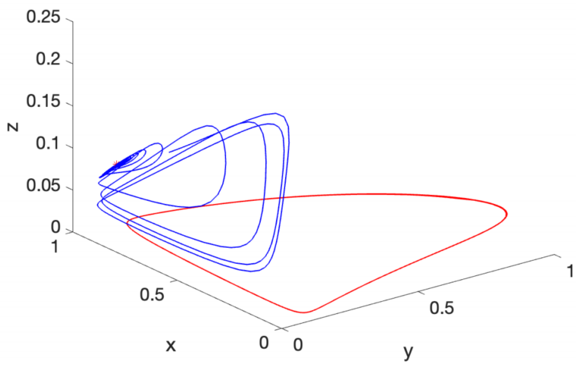

Figure 7. Coexisting stable equilibrium and limit cycle of Equation (3) with $(K, m_1, c_1, c_2, c_3, B, d_1, d_2) = (5, 1, 1.2, 1.1, 1, 1, 0.1, 0.2)$ and $m_2 = 55$.

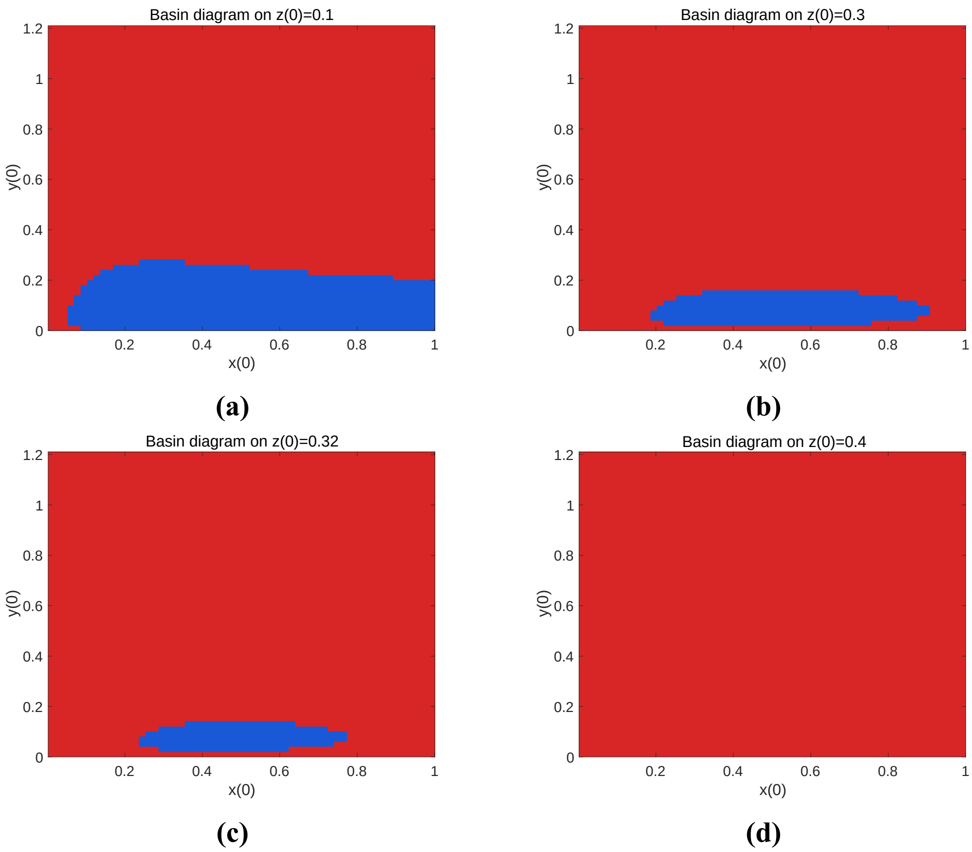

Figure 8. Basin-of-attraction on some two-dimensional sections of the initial-condition space: **(a)** $z(0) = 0.1$; **(b)** $z(0) = 0.3$; **(c)** $z(0) = 0.34$; **(d)** $z(0) = 0.4$. The grid size is 60×60.

5.2.2. The coexistence of two stable limit cycles

Let $(K, m_1, c_1, c_2, c_3, B, d_1, d_2) = (5, 1, 1.2, 1.1, 1, 1, 0.1, 0.2)$ and $m_2 = 45$. In this case, Equation (3) has a unique interior equilibrium $(0.8565, 0.02487, 0.09880)$, and the corresponding eigenvalues are $-0.1241, 0.0005667 \pm 0.04343\mathrm{i}$. This implies that the unique interior equilibrium is unstable. Moreover, we find that the system could have coexistence of two stable limit cycles Γ_1 (red colour) and Γ_2 (green colour), see **Figure 9**, where the initial points are $(0.8, 0.2, 0.1)$ and $(0.5, 0.5, 0.1)$, respectively.

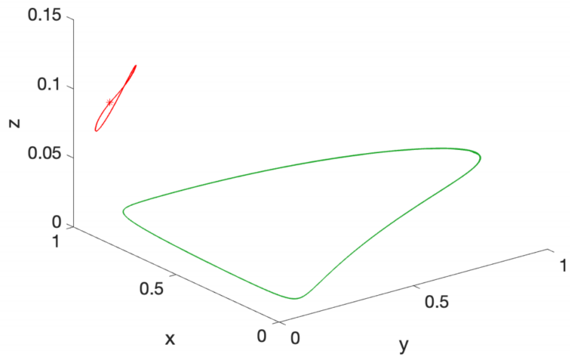

Figure 9. Two coexisting stable limit cycles of Equation (3) with $(K, m_1, c_1, c_2, c_3, B, d_1, d_2) = (5, 1, 1.2, 1.1, 1, 1, 0.1, 0.2)$ and $m_2 = 45$.

Figure 10 presents basin-of-attraction diagrams on four two-dimensional initial-condition sections. The red and green regions correspond to initial conditions converging to stable limit cycles Γ_1 and Γ_2, respectively. For $z(0) = 0.1$, the basin of stable limit cycle Γ_1 occupies a relatively large portion of the lower part of the $(x(0), y(0))$-plane. As $z(0)$ increases, this basin contracts and becomes increasingly localized. At $z(0) = 0.44$, only a small set of initial conditions with moderate $x(0)$ and low $y(0)$ converges to stable limit cycle Γ_1. For $z(0) = 0.5$, all sampled initial conditions on the considered section converge to the stable limit cycle Γ_2. These results demonstrate that the relative basin sizes of the two coexisting periodic attractors depend strongly on the initial density of the top predator. In particular, within the initial-condition region examined here, increasing $z(0)$ favors convergence to stable limit cycle Γ_2.

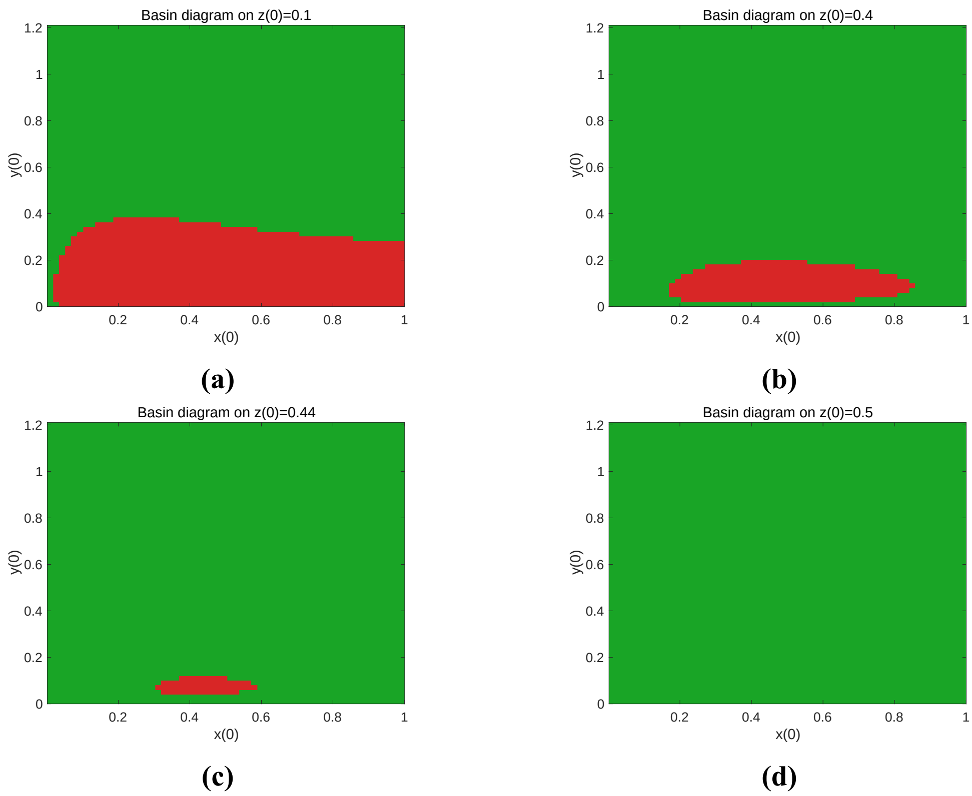

Figure 10. Basin-of-attraction on some two-dimensional sections of the initial-condition space: **(a)** $z(0) = 0.1$; **(b)** $z(0) = 0.4$; **(c)** $z(0) = 0.44$; **(d)** $z(0) = 0.5$. The grid size is 60×60.

5.3. Chaotic attractor

Let $(K, m_2, c_1, c_2, c_3, B, d_1, d_2) = (5, 10, 1.2, 1.1, 1, 1, 0.1, 0.2)$ and vary $m_1 \in [0.1, 30]$. The largest Lyapunov exponent diagram and bifurcation diagram is given in **Figure 11**, where $x = 0.8$ is the cross section.

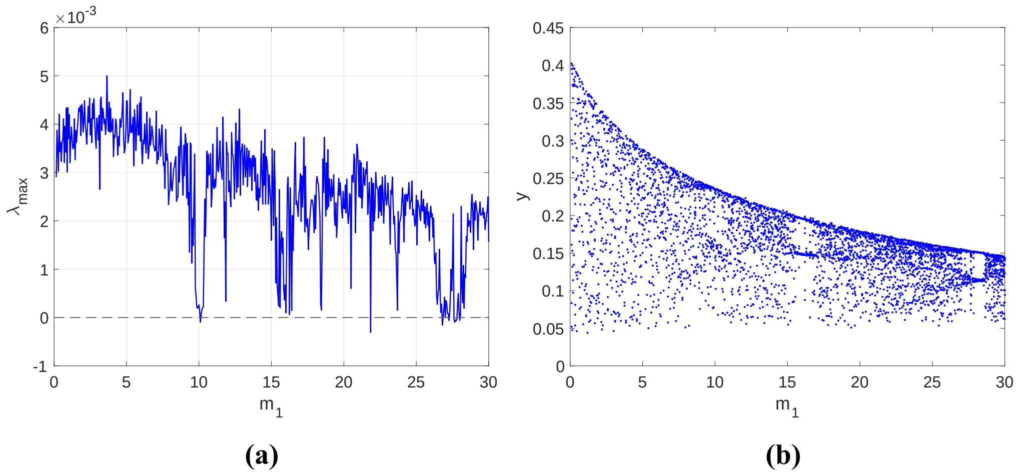

Figure 11. Equation (3) with $(K, m_2, c_1, c_2, c_3, B, d_1, d_2) = (5, 10, 1.2, 1.1, 1, 1, 0.1, 0.2)$ and $m_1 \in [0.1, 30]$: **(a)** largest Lyapunov exponent diagram; **(b)** bifurcation diagram.

As $m_1 = 1$, Equation (3) has a unique interior equilibrium $(0.9526, 0.02040, 0.1004)$, and the corresponding eigenvalues are $-0.4489, 0.004131 \pm 0.03960\mathrm{i}$. This implies that the unique interior equilibrium is unstable. Moreover, we find that the system with the unique unstable interior equilibrium could show a chaotic attractor, see **Figure 12**.

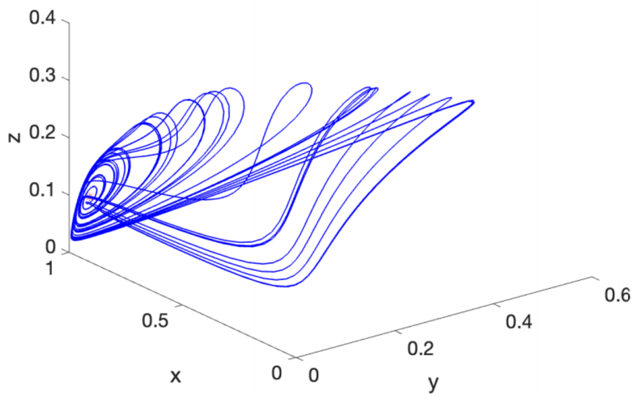

Figure 12. The chaotic attractor of system (3) with $(K, m_2, c_1, c_2, c_3, B, d_1, d_2) = (5, 10, 1.2, 1.1, 1, 1, 0.1, 0.2)$ and $m_1 = 1$.

As $m_1 = 20$, the system (3) has two interior equilibria $(0.1915, 0.2073, 0.03550)$ and $(0.9428, 0.02081, 0.1002)$. The corresponding eigenvalues are $0.01191, 0.01741 \pm 0.1274\mathrm{i}$ and $-0.3670, 0.003777 \pm 0.03948\mathrm{i}$, respectively. This implies that the two interior equilibria are unstable. Moreover, we find that the system with two unstable interior equilibria could show a chaotic attractor, see **Figure 13**.

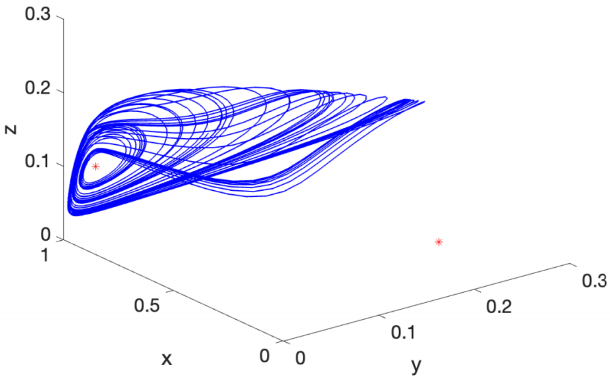

Figure 13. The chaotic attractor of system (3) with $(K, m_2, c_1, c_2, c_3, B, d_1, d_2) = (5, 10, 1.2, 1.1, 1, 1, 0.1, 0.2)$ and $m_1 = 20$.

6. Conclusion

In this paper, we investigated a tri-trophic predator-prey system with double fear effects, in which the basal prey is affected by fear induced by both the intermediate predator and the top predator. The top predator is allowed to feed on both the basal prey and the intermediate predator, which makes the trophic interaction structure more flexible than a simple food-chain model.

We first analyzed the existence of axial equilibria and obtained sufficient conditions for their global stability. These results describe the possible extinction or partial survival states of the system. Then, we studied the number and local stability of interior equilibria, which correspond to the coexistence of all three species. Hopf bifurcations were further investigated, and the first Lyapunov coefficient was computed to determine the direction of the bifurcation and the stability of the bifurcating periodic solutions. Numerical simulations revealed richer dynamical behaviors, including period-three limit cycles, non-attracting chaotic sets, coexistence of a stable equilibrium and a stable limit cycle, coexistence of two stable limit cycles, and chaotic attractors under parameter regimes with different numbers of interior equilibria.

From an ecological point of view, these results indicate that double effects can substantially influence the long-term dynamics of the system. Within the particular parameter regimes examined in this study, variations in fear intensity may move the system across a Hopf bifurcation or into regions characterized by periodic oscillations, multistability, or chaotic dynamics. This observation is parameter-dependent and should not be interpreted as a universal monotone relationship between fear intensity and ecosystem stability. The coexistence of multiple attractors also has an important ecological implication. Under the same parameter values, different initial species densities may lead to qualitatively different long-term outcomes, such as convergence to a stable equilibrium, or to one of several persistent oscillatory states. In particular, chaotic attractors imply that long-term prediction of population densities may become difficult, even though the system is deterministic.

Overall, the study shows that double fear effects are not merely passive modifications of prey growth, but can serve as key mechanisms generating complex dynamical transitions in tri-trophic ecological systems. These findings highlight the importance of considering both direct predation and fear-mediated indirect effects when modeling population interactions across multiple trophic levels.

Author contributions: Conceptualization, TY and YC; methodology, TY and YC; software, TY; validation, TY; investigation, TY; writing—original draft preparation, TY; writing—review and editing, YC; visualization, TY; supervision, YC. Both authors have read and agreed to the published version of the manuscript.

Funding: This work was supported by the Jiangxi Provincial Natural Science Foundation (Nos. 20242BAB20005 and 20252BAC200151).

Institutional review board statement: Not applicable.

Informed consent statement: Not applicable.

Data availability statement: No new data was used for the research described in the article.

Conflict of interest: The authors declare no conflict of interest.

AI use statement: The authors declare that no artificial intelligence (AI) tools were used in the preparation of this manuscript.

References

1. Lotka AJ. Elements of Physical Biology. Williams & Wilkins; 1925.
2. Volterra V. Variations and Fluctuations in the Number of Individuals in Coexisting Animal Species. Leonardo da Vinci Printing Company; 1926. (in Italian)
3. Holling CS. The components of predation as revealed by a study of small-mammal predation of the European pine sawfly. Canadian Entomologist. 1959; 91(5): 293–320.
4. May RM. Stability and Complexity in Model Ecosystems. Princeton University Press; 2001.
5. Zhang L, Wang ZC. Spatial dynamics of a diffusive predator–prey model with stage structure. Discrete and Continuous Dynamical Systems–Series B. 2015; 20(6): 1831–1853.
6. Guin LN, Pal PJ, Alzahrani J, et al. Influence of Allee effect on the spatiotemporal behavior of a diffusive predator–prey model with Crowley–Martin type response function. Scientific Reports. 2023; 13: 4710.
7. Pandey S, Ghosh U, Das D, et al. Rich dynamics of a delay-induced stage-structure prey–predator model with cooperative behaviour in both species and the impact of prey refuge. Mathematics and Computers in Simulation. 2024; 216: 49–76.
8. Shao Y, Yu H, Jin C, et al. Dynamics analysis of a predator–prey model with Allee effect and harvesting effort. Electronic Research Archive. 2024; 32(9): 5682–5716.
9. Ge J, Ji W, Liu M. Threshold behavior of a stochastic predator–prey model with fear effect and regime-switching. Applied Mathematics Letters. 2025; 164: 109476.
10. Paul B, Sikdar GC, Ghosh U. Effect of fear and non-linear predator harvesting on a predator–prey system in presence of environmental variability. Mathematics and Computers in Simulation. 2025; 227: 442–460.
11. Qi H, Jin J, Liu B, et al. Stationary distribution of a stochastic reaction–diffusion predator–prey model with additional food, fear effect and anti-predator behavior. Applied Mathematics Letters. 2025; 169: 109612.
12. Hastings A, Powell T. Chaos in a three-species food chain. Ecology. 1991; 72(3): 896–903.
13. Klebanoff A, Hastings A. Chaos in three-species food chains. Journal of Mathematical Biology. 1994; 32(5): 427–451.
14. Ramasamy S, Banjerdpongchai D, Park P. Chaos control of a delayed tri-trophic food chain model with fear and its carry over effects. Symmetry. 2023; 15(2): 484.
15. Qin W, Dong Z. The impact of resource limitation on the pest-natural enemy ecosystem with anti-predator behavior and fear effect. Advances in Continuous and Discrete Models. 2024; 2024: 10.

16. Brown JS, Laundré JW, Gurung M. The ecology of fear: Optimal foraging, game theory, and trophic interactions. Journal of Mammalogy. 1999; 80(2): 385–399.
17. Preisser EL, Bolnick DI, Benard MF. Scared to death? The effects of intimidation and consumption in predator–prey interactions. Ecology. 2005; 86(2): 501–509.
18. Zanette LY, White AF, Allen MC, et al. Perceived predation risk reduces the number of offspring songbirds produce per year. Science. 2011; 334(6061): 1398–1401.
19. Wang X, Zanette L, Zou X. Modelling the fear effect in predator–prey interactions. Journal of Mathematical Biology. 2016; 73(5): 1179–1204.
20. Kumar A, Dubey B. Modeling the effect of fear in a prey–predator system with prey refuge and gestation delay. International Journal of Bifurcation and Chaos. 2019; 29(14): 1950195.
21. Wang X, Zou X. Modeling the fear effect in predator–prey interactions with adaptive avoidance of predators. Bulletin of Mathematical Biology. 2017; 79(6): 1325–1359.
22. Pal S, Pal N, Samanta S, et al. Fear effect in prey and hunting cooperation among predators in a Leslie–Gower model. Mathematical Biosciences and Engineering. 2019; 16(5): 5146–5179.
23. Panday P, Pal N, Samanta S, et al. Stability and bifurcation analysis of a three-species food chain model with fear. International Journal of Bifurcation and Chaos. 2018; 28(1): 1850009.
24. Cong P, Fan M, Zou X. Dynamics of a three-species food chain model with fear effect. Communications in Nonlinear Science and Numerical Simulation. 2021; 99: 105809.
25. Kumar V, Kumari N. Controlling chaos in three-species food chain model using fear effect. AIMS Mathematics. 2020; 5(2): 828–842.
26. Rana S, Bhattacharya S, Samanta S. Complex dynamics of a three-species food chain model with fear and Allee effect. International Journal of Bifurcation and Chaos. 2022; 32(10): 2250084.
27. Hsu SB, Ruan S, Yang TH. Analysis of three-species Lotka–Volterra food web models with omnivory. Journal of Mathematical Analysis and Applications. 2015; 426(1): 659–687.
28. Kratina P, LeCraw RM, Ingram T, et al. Stability and persistence of food webs with omnivory: Is there a general pattern? Ecosphere. 2012; 3(6): 50.
29. Arancibia-Ibarra C, Flores J. Dynamics of a Leslie–Gower predator–prey model with Holling type II functional response, Allee effect and a generalist predator. Mathematics and Computers in Simulation. 2021; 188: 1–22.
30. Sk N, Mondal B, Sarkar A, et al. Chaos emergence and dissipation in a three-species food web model with intraguild predation and cooperative hunting. AIMS Mathematics. 2024; 9(1): 1023–1045.
31. Wang T, Wang H. Stoichiometry-dependent fear effect in a food chain model. SIAM Journal on Applied Mathematics. 2024; 84(3): 783–807.
32. Han R, Guin LN, Dai B. Consequences of refuge and diffusion in a spatiotemporal predator–prey model. Nonlinear Analysis: Real World Applications. 2021; 60: 103311.
33. Pal S, Karmakar S, Pal S, et al. Impact of fear and group defense on the dynamics of a predator–prey system. International Journal of Bifurcation and Chaos. 2024; 34(2): 2450019.
34. Cui W, Zhao Y. Bifurcation analysis of a predator–prey model with alternative prey and prey refuges. International Journal of Bifurcation and Chaos. 2024; 34(2): 2450021.
35. Din Q, Naseem RA, Shabbir MS. Predator–prey interaction with fear effects: Stability, bifurcation and two-parameter analysis incorporating complex and fractal behavior. Fractal and Fractional. 2024; 8(4): 221.
36. Saha S, Pal S, Melnik R. Analysis of the impact of fear in the presence of additional food and prey refuge with nonlocal predator–prey models. Ecological Modelling. 2025; 505: 111103.
37. Li TY, Yorke JA. Period three implies chaos. The American Mathematical Monthly. 1975; 82(10): 985–992.

Appendix A. Computation of the first Lyapunov coefficient

If $\mu = \mu^*$, we rewrite system (3) as

$$\dot{X} = F(X), \tag{A1}$$

where $X = (X_1, X_2, X_3)^{\mathrm{T}} = (x, y, z)^{\mathrm{T}}$, $F = (f_1, f_2, f_3)^{\mathrm{T}}$.

Define

$$S = 1 + m_1 y^* + m_2 z^*, \qquad H = B + Kx^*, \qquad G = B + c_1 K y^*,$$
$$L = x^*(1 - x^*), \qquad R = c_1 y^* + c_2 z^*. \tag{A2}$$

Let

$$\boldsymbol{\xi} = \begin{pmatrix} \xi_1 \\ \xi_2 \\ \xi_3 \end{pmatrix} = \begin{pmatrix} x - x^* \\ y - y^* \\ z - z^* \end{pmatrix},$$

then the obtained system has the Taylor expansion

$$\dot{\boldsymbol{\xi}} = J^* \boldsymbol{\xi} + \frac{1}{2}\mathcal{B}(\boldsymbol{\xi}, \boldsymbol{\xi}) + \frac{1}{6}\mathcal{C}(\boldsymbol{\xi}, \boldsymbol{\xi}, \boldsymbol{\xi}) + O(\|\boldsymbol{\xi}\|^4), \tag{A3}$$

where

$$[\mathcal{B}(\boldsymbol{u}, \boldsymbol{v})]_j = \sum_{k,\ell=1}^{3} \frac{\partial^2 f_j}{\partial X_k \partial X_\ell}(E^*) u_k v_\ell, \tag{A4}$$

$$[\mathcal{C}(\boldsymbol{u}, \boldsymbol{v}, \boldsymbol{w})]_j = \sum_{k,\ell,r=1}^{3} \frac{\partial^3 f_j}{\partial X_k \partial X_\ell \partial X_r}(E^*) u_k v_\ell w_r. \tag{A5}$$

Compute second-order coefficients of $[\mathcal{B}(\boldsymbol{u}, \boldsymbol{v})]_j$, write

$$\beta_{k\ell}^{(j)} = \frac{\partial^2 f_j}{\partial X_k \partial X_\ell}(E^*),$$

then for the first component,

$$\begin{aligned}
\beta_{11}^{(1)} &= -\frac{2}{S} + \frac{2BKR}{H^3}, & \beta_{12}^{(1)} &= -\frac{m_1(1 - 2x^*)}{S^2} - \frac{Bc_1}{H^2}, \\
\beta_{13}^{(1)} &= -\frac{m_2(1 - 2x^*)}{S^2} - \frac{Bc_2}{H^2}, & \beta_{22}^{(1)} &= \frac{2m_1^2 L}{S^3}, \\
\beta_{23}^{(1)} &= \frac{2m_1 m_2 L}{S^3}, & \beta_{33}^{(1)} &= \frac{2m_2^2 L}{S^3}.
\end{aligned} \tag{A6}$$

For the second component,

$$\beta_{11}^{(2)} = -\frac{2BKc_1 y^*}{H^3}, \quad \beta_{12}^{(2)} = \frac{Bc_1}{H^2}, \quad \beta_{22}^{(2)} = \frac{2Bc_1 K c_2 z^*}{G^3}, \quad \beta_{23}^{(2)} = -\frac{Bc_2}{G^2},$$
$$\beta_{13}^{(2)} = \beta_{33}^{(2)} = 0. \tag{A7}$$

For the third component,

$$\beta_{11}^{(3)} = -\frac{2BKc_2 z^*}{H^3}, \quad \beta_{13}^{(3)} = \frac{Bc_2}{H^2}, \quad \beta_{22}^{(3)} = -\frac{2Bc_1 K c_3 z^*}{G^3}, \quad \beta_{23}^{(3)} = \frac{Bc_3}{G^2},$$
$$\beta_{12}^{(3)} = \beta_{33}^{(3)} = 0. \tag{A8}$$

Then, one has

$$\begin{aligned}
[\mathcal{B}(\boldsymbol{u}, \boldsymbol{v})]_j = {} & \beta_{11}^{(j)} u_1 v_1 + \beta_{12}^{(j)}(u_1 v_2 + u_2 v_1) + \beta_{13}^{(j)}(u_1 v_3 + u_3 v_1) \\
& + \beta_{22}^{(j)} u_2 v_2 + \beta_{23}^{(j)}(u_2 v_3 + u_3 v_2) + \beta_{33}^{(j)} u_3 v_3.
\end{aligned} \tag{A9}$$

Compute third-order coefficients of $[\mathcal{C}(\boldsymbol{u},\boldsymbol{v},\boldsymbol{w})]_j$, write

$$\gamma_{k\ell r}^{(j)}=\frac{\partial^3 f_j}{\partial X_k\partial X_\ell\partial X_r}(E^*),$$

then for the first component,

$$\begin{gathered}
\gamma_{111}^{(1)}=-\frac{6BK^2R}{H^4},\quad \gamma_{112}^{(1)}=\frac{2m_1}{S^2}+\frac{2BKc_1}{H^3},\quad \gamma_{113}^{(1)}=\frac{2m_2}{S^2}+\frac{2BKc_2}{H^3},\\
\gamma_{122}^{(1)}=\frac{2m_1^2(1-2x^*)}{S^3},\quad \gamma_{123}^{(1)}=\frac{2m_1m_2(1-2x^*)}{S^3},\quad \gamma_{133}^{(1)}=\frac{2m_2^2(1-2x^*)}{S^3},\\
\gamma_{222}^{(1)}=-\frac{6m_1^3L}{S^4},\quad \gamma_{223}^{(1)}=-\frac{6m_1^2m_2L}{S^4},\quad \gamma_{233}^{(1)}=-\frac{6m_1m_2^2L}{S^4},\quad \gamma_{333}^{(1)}=-\frac{6m_2^3L}{S^4}.
\end{gathered}\tag{A10}$$

For the second component,

$$\begin{aligned}
\gamma_{111}^{(2)}&=\frac{6BK^2c_1y^*}{H^4}, & \gamma_{112}^{(2)}&=-\frac{2BKc_1}{H^3},\\
\gamma_{222}^{(2)}&=-\frac{6BK^2c_1^2c_2z^*}{G^4}, & \gamma_{223}^{(2)}&=\frac{2BKc_1c_2}{G^3}.
\end{aligned}\tag{A11}$$

For the third component,

$$\begin{aligned}
\gamma_{111}^{(3)}&=\frac{6BK^2c_2z^*}{H^4}, & \gamma_{113}^{(3)}&=-\frac{2BKc_2}{H^3},\\
\gamma_{222}^{(3)}&=\frac{6BK^2c_1^2c_3z^*}{G^4}, & \gamma_{223}^{(3)}&=-\frac{2BKc_1c_3}{G^3}.
\end{aligned}\tag{A12}$$

From

$$J^*q=\mathrm{i}\omega_0q,\qquad {J^*}^{\mathsf{T}}p=-\mathrm{i}\omega_0p,\qquad \langle p,q\rangle=\overline{p}^{\mathsf{T}}q=1,$$

one gets

$$q=(1,u,v)^{\mathsf{T}},\qquad p=\frac{1}{1+\overline{r}\,u+\overline{s}\,v}(1,r,s)^{\mathsf{T}},\tag{A13}$$

where

$$\begin{aligned}
u&=\frac{J_{23}J_{31}-J_{21}(J_{33}-\mathrm{i}\omega_0)}{(J_{22}-\mathrm{i}\omega_0)(J_{33}-\mathrm{i}\omega_0)-J_{23}J_{32}},v=\frac{J_{21}J_{32}-J_{31}(J_{22}-\mathrm{i}\omega_0)}{(J_{22}-\mathrm{i}\omega_0)(J_{33}-\mathrm{i}\omega_0)-J_{23}J_{32}},\\
r&=\frac{J_{13}J_{32}-J_{12}(J_{33}+\mathrm{i}\omega_0)}{(J_{22}+\mathrm{i}\omega_0)(J_{33}+\mathrm{i}\omega_0)-J_{23}J_{32}},s=\frac{J_{12}J_{23}-J_{13}(J_{22}+\mathrm{i}\omega_0)}{(J_{22}+\mathrm{i}\omega_0)(J_{33}+\mathrm{i}\omega_0)-J_{23}J_{32}}.
\end{aligned}\tag{A14}$$

Define

$$\mathsf{U}=\mathcal{B}(q,\overline{q})=(\mathsf{U}_1,\mathsf{U}_2,\mathsf{U}_3)^{\mathsf{T}},\qquad \mathsf{V}=\mathcal{B}(q,q)=(\mathsf{V}_1,\mathsf{V}_2,\mathsf{V}_3)^{\mathsf{T}}.$$

Then, from Equations (A6)–(A9), one has

$$\begin{aligned}
\mathsf{U}_1=&-\frac{2}{S}+\frac{2BKR}{H^3}+\left(-\frac{m_1(1-2x^*)}{S^2}-\frac{Bc_1}{H^2}\right)(u+\overline{u})\\
&+\left(-\frac{m_2(1-2x^*)}{S^2}-\frac{Bc_2}{H^2}\right)(v+\overline{v})+\frac{2m_1^2L}{S^3}u\overline{u}\\
&+\frac{2m_1m_2L}{S^3}(u\overline{v}+v\overline{u})+\frac{2m_2^2L}{S^3}v\overline{v},\\
\mathsf{U}_2=&-\frac{2BKc_1y^*}{H^3}+\frac{Bc_1}{H^2}(u+\overline{u})+\frac{2Bc_1Kc_2z^*}{G^3}u\overline{u}-\frac{Bc_2}{G^2}(u\overline{v}+v\overline{u}),\\
\mathsf{U}_3=&-\frac{2BKc_2z^*}{H^3}+\frac{Bc_2}{H^2}(v+\overline{v})-\frac{2Bc_1Kc_3z^*}{G^3}u\overline{u}+\frac{Bc_3}{G^2}(u\overline{v}+v\overline{u}),
\end{aligned}\tag{A15}$$

and

$$\begin{aligned}
\mathsf{V}_1 =& -\frac{2}{S} + \frac{2BKR}{H^3} + 2\left(-\frac{m_1(1-2x^*)}{S^2} - \frac{Bc_1}{H^2}\right)u \\
&+ 2\left(-\frac{m_2(1-2x^*)}{S^2} - \frac{Bc_2}{H^2}\right)v + \frac{2m_1^2L}{S^3}u^2 + \frac{4m_1m_2L}{S^3}uv + \frac{2m_2^2L}{S^3}v^2, \\
\mathsf{V}_2 =& -\frac{2BKc_1y^*}{H^3} + \frac{2Bc_1}{H^2}u + \frac{2Bc_1Kc_2z^*}{G^3}u^2 - \frac{2Bc_2}{G^2}uv, \\
\mathsf{V}_3 =& -\frac{2BKc_2z^*}{H^3} + \frac{2Bc_2}{H^2}v - \frac{2Bc_1Kc_3z^*}{G^3}u^2 + \frac{2Bc_3}{G^2}uv. \qquad \text{(A16)}
\end{aligned}$$

Define

$$h_{11} = -J^{*-1}\mathsf{U} = (h_1, h_2, h_3)^{\mathsf{T}}, \qquad h_{20} = (2\mathrm{i}\omega_0 I - J^*)^{-1}\mathsf{V} = (k_1, k_2, k_3)^{\mathsf{T}},$$

then

$$\begin{aligned}
h_1 &= -\frac{1}{D_{J^*}}\left[(J_{22}J_{33} - J_{23}J_{32})\mathsf{U}_1 + (J_{13}J_{32} - J_{12}J_{33})\mathsf{U}_2 + (J_{12}J_{23} - J_{13}J_{22})\mathsf{U}_3\right], \\
h_2 &= -\frac{1}{D_{J^*}}\left[(J_{23}J_{31} - J_{21}J_{33})\mathsf{U}_1 + (J_{11}J_{33} - J_{13}J_{31})\mathsf{U}_2 + (J_{13}J_{21} - J_{11}J_{23})\mathsf{U}_3\right], \\
h_3 &= -\frac{1}{D_{J^*}}\left[(J_{21}J_{32} - J_{22}J_{31})\mathsf{U}_1 + (J_{12}J_{31} - J_{11}J_{32})\mathsf{U}_2 + (J_{11}J_{22} - J_{12}J_{21})\mathsf{U}_3\right], \qquad \text{(A17)}
\end{aligned}$$

and

$$\begin{aligned}
k_1 =& \frac{1}{D_M}\big\{[(\mathrm{i}\omega_0 - J_{22})(\mathrm{i}\omega_0 - J_{33}) - J_{23}J_{32}]\mathsf{V}_1 \\
&+ [J_{13}J_{32} + J_{12}(\mathrm{i}\omega_0 - J_{33})]\mathsf{V}_2 + [J_{12}J_{23} + J_{13}(\mathrm{i}\omega_0 - J_{22})]\mathsf{V}_3\big\}, \\
k_2 =& \frac{1}{D_M}\big\{[J_{23}J_{31} + J_{21}(\mathrm{i}\omega_0 - J_{33})]\mathsf{V}_1 \\
&+ [(\mathrm{i}\omega_0 - J_{11})(\mathrm{i}\omega_0 - J_{33}) - J_{13}J_{31}]\mathsf{V}_2 + [J_{13}J_{21} + J_{23}(\mathrm{i}\omega_0 - J_{11})]\mathsf{V}_3\big\}, \\
k_3 =& \frac{1}{D_M}\big\{[J_{21}J_{32} + J_{31}(\mathrm{i}\omega_0 - J_{22})]\mathsf{V}_1 \\
&+ [J_{12}J_{31} + J_{32}(\mathrm{i}\omega_0 - J_{11})]\mathsf{V}_2 + [(\mathrm{i}\omega_0 - J_{11})(\omega - J_{22}) - J_{12}J_{21}]\mathsf{V}_3\big\}, \qquad \text{(A18)}
\end{aligned}$$

where

$$\begin{aligned}
D_{J^*} &= \det J^* = J_{11}(J_{22}J_{33} - J_{23}J_{32}) - J_{12}(J_{21}J_{33} - J_{23}J_{31}) \\
&\quad + J_{13}(J_{21}J_{32} - J_{22}J_{31}), \\
D_M &= \det M = \det(2\mathrm{i}\omega_0 I - J^*). \qquad \text{(A19)}
\end{aligned}$$

Define

$$\mathsf{P} = \mathcal{B}(\overline{q}, h_{20}) = (\mathsf{P}_1, \mathsf{P}_2, \mathsf{P}_3)^{\mathsf{T}}, \qquad \mathsf{T} = \mathcal{B}(q, h_{11}) = (\mathsf{T}_1, \mathsf{T}_2, \mathsf{T}_3)^{\mathsf{T}},$$

then

$$\begin{aligned}
\mathsf{P}_1 =& \left(-\frac{2}{S} + \frac{2BKR}{H^3}\right)k_1 + \left(-\frac{m_1(1-2x^*)}{S^2} - \frac{Bc_1}{H^2}\right)(k_2 + \overline{u}\,k_1) \\
&+ \left(-\frac{m_2(1-2x^*)}{S^2} - \frac{Bc_2}{H^2}\right)(k_3 + \overline{v}\,k_1) + \frac{2m_1^2L}{S^3}\overline{u}\,k_2 \\
&+ \frac{2m_1m_2L}{S^3}(\overline{u}\,k_3 + \overline{v}\,k_2) + \frac{2m_2^2L}{S^3}\overline{v}\,k_3, \\
\mathsf{P}_2 =& -\frac{2BKc_1y^*}{H^3}k_1 + \frac{Bc_1}{H^2}(k_2 + \overline{u}\,k_1) + \frac{2Bc_1Kc_2z^*}{G^3}\overline{u}\,k_2 \\
&- \frac{Bc_2}{G^2}(\overline{u}\,k_3 + \overline{v}\,k_2), \\
\mathsf{P}_3 =& -\frac{2BKc_2z^*}{H^3}k_1 + \frac{Bc_2}{H^2}(k_3 + \overline{v}\,k_1) - \frac{2Bc_1Kc_3z^*}{G^3}\overline{u}\,k_2 \\
&+ \frac{Bc_3}{G^2}(\overline{u}\,k_3 + \overline{v}\,k_2), \qquad \text{(A20)}
\end{aligned}$$

and

$$
\begin{aligned}
\mathsf{T}_1 =& \left(-\frac{2}{S}+\frac{2BKR}{H^3}\right)h_1+\left(-\frac{m_1(1-2x^*)}{S^2}-\frac{Bc_1}{H^2}\right)(h_2+uh_1)\\
&+\left(-\frac{m_2(1-2x^*)}{S^2}-\frac{Bc_2}{H^2}\right)(h_3+vh_1)+\frac{2m_1^2L}{S^3}uh_2\\
&+\frac{2m_1m_2L}{S^3}(uh_3+vh_2)+\frac{2m_2^2L}{S^3}vh_3,\\
\mathsf{T}_2 =& -\frac{2BKc_1y^*}{H^3}h_1+\frac{Bc_1}{H^2}(h_2+uh_1)+\frac{2Bc_1Kc_2z^*}{G^3}uh_2-\frac{Bc_2}{G^2}(uh_3+vh_2),\\
\mathsf{T}_3 =& -\frac{2BKc_2z^*}{H^3}h_1+\frac{Bc_2}{H^2}(h_3+vh_1)-\frac{2Bc_1Kc_3z^*}{G^3}uh_2+\frac{Bc_3}{G^2}(uh_3+vh_2).
\end{aligned}
\tag{A21}
$$

Define

$$\mathsf{C}=\mathcal{C}(q,q,\overline{q})=(\mathsf{C}_1,\mathsf{C}_2,\mathsf{C}_3)^{\mathsf{T}}.$$

Then, substituting the coefficients from (A10)–(A12) into (A5), one gets

$$
\begin{aligned}
\mathsf{C}_1 =& -\frac{6BK^2R}{H^4}+\left(\frac{2m_1}{S^2}+\frac{2BKc_1}{H^3}\right)(2u+\overline{u})\\
&+\left(\frac{2m_2}{S^2}+\frac{2BKc_2}{H^3}\right)(2v+\overline{v})+\frac{2m_1^2(1-2x^*)}{S^3}(u^2+2u\overline{u})\\
&+\frac{4m_1m_2(1-2x^*)}{S^3}(uv+u\overline{v}+v\overline{u})+\frac{2m_2^2(1-2x^*)}{S^3}(v^2+2v\overline{v})\\
&-\frac{6m_1^3L}{S^4}u^2\overline{u}-\frac{6m_1^2m_2L}{S^4}(u^2\overline{v}+2uv\overline{u})\\
&-\frac{6m_1m_2^2L}{S^4}(v^2\overline{u}+2uv\overline{v})-\frac{6m_2^3L}{S^4}v^2\overline{v},\\
\mathsf{C}_2 =& \frac{6BK^2c_1y^*}{H^4}-\frac{2BKc_1}{H^3}(2u+\overline{u})-\frac{6BK^2c_1^2c_2z^*}{G^4}u^2\overline{u}\\
&+\frac{2BKc_1c_2}{G^3}(u^2\overline{v}+2uv\overline{u}),\\
\mathsf{C}_3 =& \frac{6BK^2c_2z^*}{H^4}-\frac{2BKc_2}{H^3}(2v+\overline{v})+\frac{6BK^2c_1^2c_3z^*}{G^4}u^2\overline{u}\\
&-\frac{2BKc_1c_3}{G^3}(u^2\overline{v}+2uv\overline{u}).
\end{aligned}
\tag{A22}
$$

Define

$$\mathsf{W}_j=\mathsf{C}_j+\mathsf{P}_j+2\mathsf{T}_j,\qquad j=1,2,3. \tag{A23}$$

Then the cubic resonant coefficient is

$$G_{21}=\left\langle p,\,\mathcal{C}(q,q,\overline{q})+\mathcal{B}(\overline{q},h_{20})+2\mathcal{B}(q,h_{11})\right\rangle,$$

and the first Lyapunov coefficient is

$$l_1=\frac{1}{2\omega_0}\operatorname{Re}G_{21}=\frac{1}{2\omega_0}\operatorname{Re}\left[\frac{\mathsf{W}_1+\overline{r}\,\mathsf{W}_2+\overline{s}\,\mathsf{W}_3}{1+\overline{r}\,u+\overline{s}\,v}\right]. \tag{A24}$$

Equations (A2)–(A22), substituted successively into Equation (A23) and then into Equation (A24), give an exact expression

$$l_1=l_1(x^*,y^*,z^*,\mu^*;B,K,c_1,c_2,c_3,d_1,d_2,m_1,m_2)\,.$$